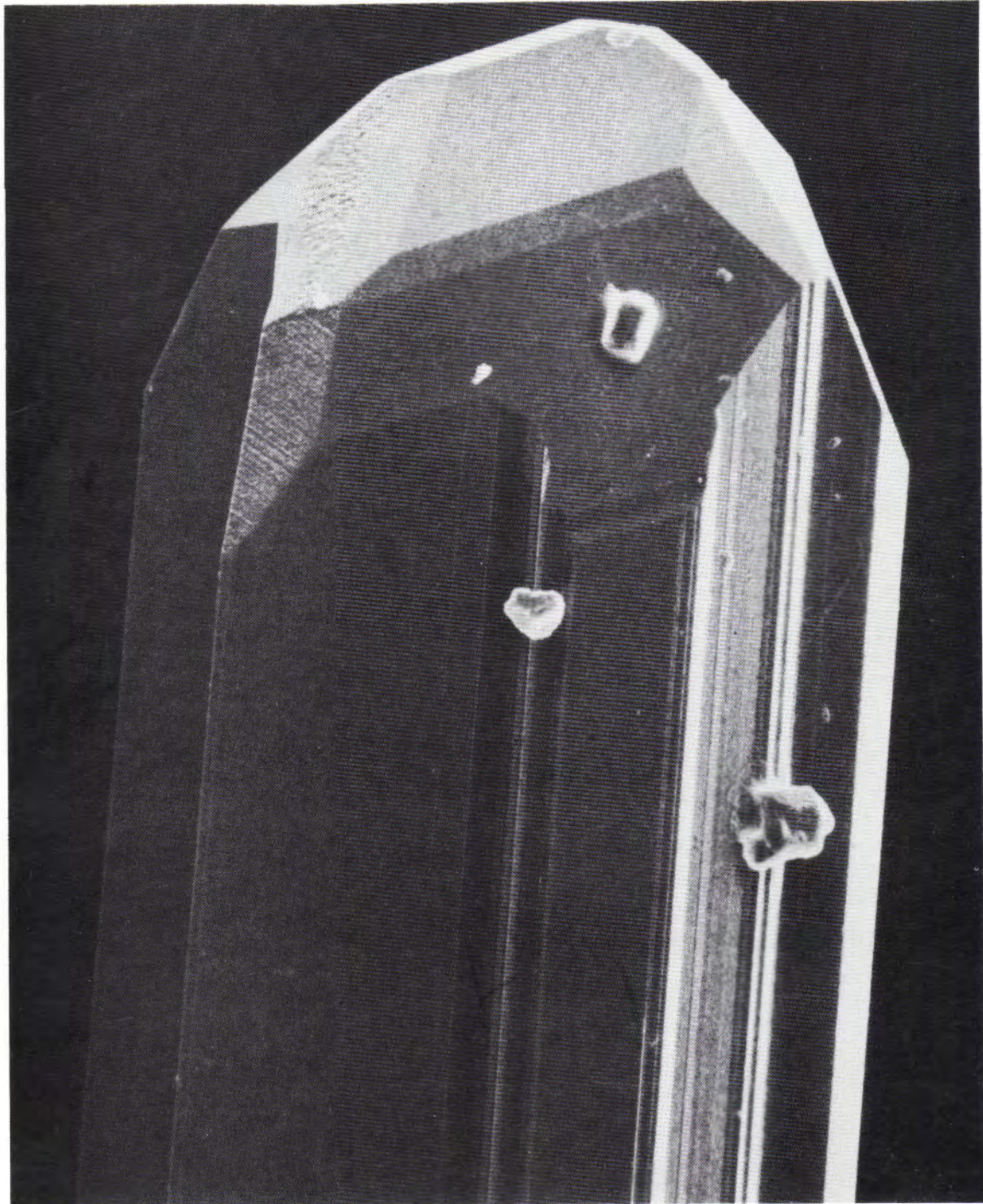


THE PICKING TABLE

JOURNAL OF THE FRANKLIN-OGDENSBURG MINERALOGICAL SOCIETY, INC.



VOLUME 35 NUMBER 1

SPRING/SUMMER 1994

\$7.50

THE FRANKLIN-OGDENSBURG MINERALOGICAL SOCIETY, INC.

OFFICERS AND STAFF

PRESIDENT

Chester S. Lemanski, Jr. 309 Massachusetts Avenue, Browns Mills, NJ 08015

FIRST VICE PRESIDENT

Lee Lowell 53 Foxtail Lane, Hamburg, NJ 07419

SECOND VICE PRESIDENT

George Elling 758 Charnwood Drive, Wykoff, NJ 07481

SECRETARY

Tema Hecht 600 West 111th Street, New York, NY 10025

TREASURER

John Cianciulli 60 Alpine Road, Sussex, NJ 07461

ASSISTANT TREASURER

Stephen C. Misiur 309 Fernwood Terrace, Linden, NJ 07036

SLIDE COLLECTION CUSTODIAN

Edward H. Wilk 202 Boiling Springs Avenue, East Rutherford, NJ 07073

TRUSTEES

John L. Baum (1994)
Philip P. Betancourt (1994)
Richard C. Bostwick (1993)
Joseph Cilen (1993)
John C. Ebner (1993)
William Kroth (1994)
Steven M. Kuitems (1993)
Warren A. Langill (1994)
Edward H. Wilk (1994)

COMMITTEE CHAIRPERSONS

Auditing	William J. Trost
Banquet	Maureen E. Woods
Field Trip	Edward H. Wilk, Warren Cummings (assistant)
Historical	John L. Baum
Identification	Richard C. Bostwick
Mineral Exchange	Richard C. Bostwick
Nominating	Philip P. Betancourt
Program	Lee Lowell
Spring Swap & Sell	Chester S. Lemanski, Jr.

LIAISON WITH THE EASTERN FEDERATION OF MINERAL AND LAPIDARY SOCIETIES (EFMLS)

Delegate Philip P. Betancourt
Alternates Richard C. Bostwick and Omer S. Dean

MEMBERSHIP INFORMATION:

Anyone interested in the minerals, mines, or mining history of the Franklin-Ogdensburg, New Jersey area is invited to join the Franklin-Ogdensburg Mineralogical Society, Inc. Membership includes scheduled meetings, lectures and field trips; as well as a subscription to *The Picking Table*. Dues are \$10 for individual and \$15 for family memberships. Please make check or money order payable to **FOMS**, and send to:

Mr. John Cianciulli, Treasurer FOMS
60 Alpine Road
Sussex, NJ 07461



THE PICKING TABLE

EDITOR

Herb Yeates
P.O. Box 46
White Plains, NY 10605

EDITORIAL BOARD

John L. Baum
Richard C. Bostwick
Omer S. Dean
Earl R. Verbeek

The Picking Table is published twice each year, in March and September, by the Franklin-Ogdensburg Mineralogical Society, Inc. (FOMS), a non-profit organization.

The Picking Table is the official journal of the FOMS, and publishes articles of interest to the mineralogical community which pertain to the Franklin-Ogdensburg, New Jersey area.

Articles related to the minerals or mines of the district are welcome for publication in *The Picking Table*. Prospective authors should contact the editor at the address listed above for further information.

Subscription to *The Picking Table* is included with membership in the FOMS. For membership, back-issue, and information on available publications see the opposite page and the inside back cover.

The views and opinions expressed in *The Picking Table* do not necessarily reflect those of the FOMS, the editor, or the editorial board.



THE PICKING TABLE

JOURNAL OF THE FRANKLIN-OGDENSBURG MINERALOGICAL SOCIETY, INC.

VOLUME 35

NUMBER 1



SPRING/SUMMER 1994

C O N T E N T S

ARTICLES

The famous late-stage oxysalt minerals of Franklin-Ogdensburg: (Part I) Closest-packing and oxidation-reduction 4
P. B. Moore

Geology and mineralogy of a veinlet assemblage associated with wollastonite-bearing rocks, Sterling Mine, Ogdensburg, New Jersey 16
R. E. Jenkins II

COLUMNS

From the Editor's Desk 2

Spring 1994 Activity Schedule 2
Meetings

ABOUT THE COVER PHOTOGRAPH

Willemite crystal. Franklin, NJ. A close-up view of the termination of a pale-green, transparent willemite crystal. Note the uneven development of crystal faces, typical of such natural crystals. The crystal is from a secondary tephroite assemblage, and is brilliantly fluorescent under shortwave ultraviolet radiation. SEM photomicrograph. Field width 0.15 mm.

FROM THE EDITOR'S DESK

Herb Yeates
P.O. Box 46
White Plains, NY 10605

IN THIS ISSUE

Professor Paul B. Moore has provided *The Picking Table* with a fascinating look at some fundamental structural and chemical properties of Franklin-Sterling minerals. A "Part II" of this work, applying some of the crystal-chemical principles discussed to specific species, should be forthcoming in the PT. You are strongly encouraged to go out and buy some ping-pong balls and work at visualizing the relationships discussed. The effort can be very rewarding.

Scientific study of the minerals found at Sterling Hill continues, and Dr. Jenkins has kindly provided us with yet another fine article sharing some of his recent work. The original manuscript included several color photographs of hand specimens. Unfortunately, they won't reproduce well here and so do not appear. Perhaps one day we will see a color PT.

We are indeed fortunate to have these scientists share their work with us through *The Picking Table*. We owe them a debt of thanks.

LOCAL NOTES

In last issue's Editor's column, I finally printed copy deadlines for our regular contributors (i.e. the FOMS President, Field trip and Speaker chairpersons, local museum staff etc.). Surprisingly, no one submitted anything by the published Spring closing date (Dec. 15). As such, even though there is plenty going on at both Franklin and Sterling Hill, thanks to the poor response you can't read about it here. Solution? Get up to Franklin and Sterling Hill and see for yourself!

A NEW EDITOR

This issue marks my two-year anniversary as Editor for *The Picking Table*. As discussed previously, it will be my last. Joe Kaiser has kindly stepped forward to serve as your next Editor.

The term has been very rewarding. I would like to thank those who have really pitched in to make these past four issues possible. You know who you are. Thank you! See you in Franklin or up at the Hill.



SPRING 1994 ACTIVITY SCHEDULE

Saturday, March 19th 1994

Field Trip — to be announced by flyer

1:30 - 3:30 — *Lecture* — Mr. Mead Stapler, "Iron Masters of Ringwood, New Jersey."

Saturday, April 16th, 1994

Field Trip — to be announced by flyer

1:30 - 3:30 — *Lecture* — Dr. Herbert Kraft, "Pahaquarry - Old Mine Road: Fact or Fiction."

Saturday, May 21st, 1994

Field Trip — to be announced by flyer

1:30 - 3:30 — *Lecture* — Mr. Manny Robbins, "The Silver of Laurion: Silver Mining, Methods and Archaeology of the Greek World."

Saturday, June 18th, 1994

Field Trip — to be announced by flyer

1:30 - 3:30 — *Lecture* — Mr. Steven Misiur, "Sterling Hill Activities."

Scheduled activities of the Society include meetings/lecture programs and field trips. The regular meetings are held on the third Saturday of March, April, May, June, September, October and November. Business meetings follow the lecture programs listed. Field trips are generally held on the weekend of a meeting/lecture program. Unless specified otherwise, all meetings/lectures are held in Kraissl Hall of the Franklin Mineral Museum, Evans Road, Franklin, New Jersey.

The Franklin Mineral Museum

Evans Road P.O. Box 54, Franklin, NJ 07416
(between Main Street and Buckwheat Road)
Phone: (201) 827-3481

Exhibiting by means of guided tours Franklin-Sterling Hill mineral specimens, educational exhibits in mining methods and history including a life-sized replica of underground working, artifacts, gem stones, zinc uses, and a 32 foot long fluorescent display. Included in the tours is the Jensen Memorial Hall built especially to contain the Wilfred Welsh collections of native American relics, fossils, and world-wide minerals and rock specimens assembled for teaching purposes.

Mineral collecting on the Buckwheat Dump. Ample parking, and picnic grounds.

Offering for sale: Minerals, fluorescent specimens, micromounts, mineral sets, amethyst crystal groups, agate slabs, onyx carvings, UV lamps, hammers, lenses, mineral books, 35mm slides of fluorescent minerals by Henry van Lenten, T-shirts, patches, postcards, dinosaur models, crystal growing kits and refreshments.

Operating Schedule:

Open to the public

March 1 to December 1

Monday through Saturday: 10AM - 4 PM

Sunday: 12:30 PM - 4:30 PM

Closed: Easter, July 4th and Thanksgiving

Groups by reservation, please

Admission fees:

Adults: \$4.00

Grammar & High School Students: \$2.00

Separate admission fee to the Buckwheat Dump is the same as the Mineral Museum fee. Admission to museum includes guided tour.

Franklin, New Jersey
"The Fluorescent Mineral
Capital of the World"



The Sterling Hill Mining Museum, Inc.



30 Plant Street Ogdensburg, NJ 07439
Museum phone: (201) 209-7212

Don't miss the RAINBOW ROOM!

Featuring 30 acres of things to see indoors, outdoors and underground, including:

- Antique mining equipment displays
- Mining memorabilia displays
- Historical buildings
- Underground guided tours
- Gift Shop - stocked with minerals, books, T-shirts, caps etc.
- Food concession and picnic area,
- Nature trails, and much more!

Learn about the importance of the mining industry to northwestern New Jersey.
See historic mine workings!

Schedule of operation:

7-days-a-week 10A.M. to 5P.M.

(last tour at 3:30P.M.)

March 1 — December 1

Admission prices:

Adults: \$6.50

Children: \$4.50

Senior Citizens: \$5.50

Call for group rates

Note:

On the last Sunday of each month (or other times for groups by prior arrangement) a collecting site will be open for a nominal additional fee. Contact the mine office for details.

THE FAMOUS LATE-STAGE OXYSALT MINERALS OF FRANKLIN-OGDENSBURG: CLOSEST-PACKING AND OXIDATION-REDUCTION

Paul B. Moore

Department of the Geophysical Sciences
University of Chicago
Chicago, Illinois 60637

INTRODUCTION

Among the Franklin-Ogdensburg (FO) mineral legacy are those “peculiar” minerals which made the localities famous world-wide. These are the late-stage or “crack” minerals a.k.a. fissure minerals or secondary products of hydrothermal refluxing. Such phases formed after the apex of regional metamorphism, but the gap in time is not known because age-dating in such a system is difficult. These crack minerals could have appeared tens or hundreds of millions of years later than the ores. Most of them were derived from the reworking of earlier primary phases such as franklinite (Zn, Mn, Fe), willemite (Zn, Mn, Si), zincite (Zn, Mn), lollingite (As, Fe), arsenopyrite (Fe, As, S), and fluoborite, (Mg, F, B). The chemistry of the primary ores is reflected in the chemistry of the crack minerals, many of which crystallized sequentially (the paragenesis) anywhere from 800° C to room temperature. I would intuit that most of the phases of great interest crystallized around or below 250° C — relatively cool geologically speaking. The primary arsenide lollingite and sulfarsenide arsenopyrite crystallized throughout the Franklin Marble (FM), especially in coarse-grained albite-quartz pegmatites and in the basic FM abutting these acid rocks.

Indeed, the arsenides were among the first minerals documented from the FM. Numerous pits, the relics of mineralogical activity in the 1830s, still can be found around the impressive Mts. Adam and Eve near Edenville, Orange County, New York, in the north-easterly extension of the FM. The pits are usually in FM where cast-off chunks of pargasitic grains of lollingite and arsenopyrite intergrowths. Three years ago I uncovered magnificent specimens of abundant coarse sprays and crystals of lollingite and arsenopyrite which make attractive displays against white albite and gray quartz. The association is abundant and far superior to anything the earlier mineralogists found.

Evidently, no one even bothered to hit the pegmatite with a crackhammer, but instead stuck to the amphiboles and the FM. On the southeast flank of Mt. Eve (a hornblende granite), one progresses easterly over about 100 feet above peaty “drowned lands,” then to a steep 50 foot ascent up pegmatite which continues easterly for about another 50 feet, beyond which is the FM. My hypothesis is that the arsenic originated from the granites and crystallized as arsenides in the pegmatite aureole, the latter a typical but rather “dry” fractionation from the earlier intruded granites. This is reminiscent of the lollingite occurrences in more

F-O Closest-Packed Structures

For Pauling $rO^{2-} = 1.40\text{\AA}$, $V_0 = 15.5\text{\AA}^3$

* - Discussed in detail.

† - Known only from Franklin-Ogdensburg

SPECIES	FORMULA	STACK	$V_0(\text{\AA}^3)$
Manganosite	${}^6\text{MnO}$ $h = 2:56\text{\AA}$. c c c .	21.9 \AA^3
*Zincite	${}^4\text{ZnO}$ $h = 2:59\text{\AA}$. h h .	23.7
*Pyrochroite	${}^6\text{Mn}(\text{OH})_2$ $h = 2:34\text{\AA}$. h h .	22.8
<u>${}^6\text{Zn}, {}^6\text{Mn}, {}^4\text{Zn}, {}^6\text{Mn}$</u>			
Chalcophanite	${}^6\text{Zn}_2(\text{H}_2\text{O})_6 \square [{}^6\text{Mn}_3{}^4\text{O}_7]_2$	3 (-chh)	16.3 (incl. \square)
Hydrozincite	$[{}^6\text{Zn}_3\text{O}_2 {}^4\text{Zn}_2\text{O}_2(\text{OH})_6]^{4-} [\text{C}_2\text{O}_2]^{4+}$.CABC. sheet	19.0
†Sclarite	$[{}^6\text{Zn}_4\text{O}_2(\text{OH})_4 {}^4\text{Zn}_2\text{O}_2(\text{OH})_6]^{6-} [{}^4\text{Zn}_2\text{C}_2\text{O}_2]^{6+}$.CABC. sheet	20.5
Flinkite	$[\text{Mn}_2^{2+}(\text{OH})_4\text{Mn}^{3+} {}^4\text{AsO}_4]$.chch.	20.5
Synadelphite	${}^6\text{Mn}_9(\text{OH})_9(\text{H}_2\text{O})_2 [{}^4\text{As}_2{}^{5+} {}^3\text{As}^{3+} \text{O}_{11}\psi]^{9-}$.chch.	21.8 (incl. ψ)
Hematolite	$[{}^6\text{Mn}_{13}\text{Al}_2(\text{OH})_{23}]^{9+} [{}^4\text{As}_2{}^{5+} {}^3\text{As}^{3+} \text{O}_{11}\psi]^{9-}$	3 (-hhhch-)	20.7 (incl. ψ)
<u>${}^4\text{Zn}, {}^6\text{Mn}$ only</u>			
†Yeatmanite	${}^6[\text{Mn}_5\text{Sb}_2] {}^4[\text{Mn}_2\text{Zn}_8\text{Si}_4\text{O}_{28}]^{20-}$.hhcc.	19.8
*Hemimorphite	${}^4[\text{Zn}_4(\text{OH})_2\text{Si}_2\text{O}_7] \cdot \text{H}_2\text{O}$.hhhh.	23.0
††Hodgkinsonite	${}^6\text{Mn}(\text{OH})_2 {}^4[\text{Zn}_2\text{SiO}_4]$.hhhhhh.	21.2
††Holdenite	${}^6\text{Mn}_6(\text{OH})_2 {}^4[\text{Zn}(\text{OH})_4] {}^4[\text{Zn}_2\text{As}_2\text{SiO}_{12}(\text{OH})_2]^{8-}$.cccccc.	20.5
††Kolicite	${}^6\text{Mn}_7(\text{OH})_4 {}^4[\text{Zn}_4\text{As}_2\text{Si}_2\text{O}_{16}(\text{OH})_4]^{10-}$.cccccc.	20.5
*Clinohedrite	${}^6\text{Ca}(\text{H}_2\text{O}) {}^4[\text{ZnSiO}_4]^{2-}$.cccccc.	21.1
*Junitoite	${}^6\text{Ca} {}^4[\text{Zn}_2\text{Si}_2\text{O}_7]^{2-} \cdot \text{H}_2\text{O}$.cccccc.	21.1
††Gerstmannite	${}^6\text{MnMg}(\text{OH})_2 {}^4[\text{ZnSiO}_4]^{2-}$.cccccc.	19.9
Loseyite	$[{}^6\text{Mn}_4\text{O}_2(\text{OH})_4 {}^4\text{Zn}_2\text{O}_2(\text{OH})_6]^{6-} [{}^4\text{Zn}_2\text{C}_2\text{O}_2]^{6+}$.CABC-sheet	21.4
†Lawsonbauerite	$[{}^6\text{Mn}_7(\text{OH})_6 {}^4\text{Zn}_4(\text{OH})_{16}] \cdot [{}^6\text{Mn}_2(\text{H}_2\text{O})_8(\text{SO}_4)_2]$.CABC-sheet	21.8
†Mooreite	$[{}^6\text{Mg}_9(\text{OH})_{10} {}^4\text{Zn}_4(\text{OH})_{16}] \cdot [{}^6\text{Mn}_2(\text{H}_2\text{O})_8(\text{SO}_4)_2]$.CABC-sheet	22.1
	mean (excluding Mn^{4+})		21.3 \AA^3
	range (" ")		19.0 - 23.7 \AA^3

Table 1. Franklin-Ogdensburg Closest-Packed Structures.

Nearly all these phases are crack minerals. Coordination numbers are shown as superscripts. Structural packages are in brackets.

aqueous pegmatites around Harney Peak granite in the Black Hills in South Dakota; and the pegmatites associated with the Keene and Concord granites in New Hampshire. We presently know that the granite and its pegmatite of Mt. Eve are of very similar ages, or about 1,000 Ma. These ages were obtained from U/Pb age dates in primary zircons.

I belabor this point because I believe FO were initially closed systems and that nearly all minerals there were derived from refluxing of primary phases through fluids in relatively small cracks. The FO system is rather dry; volumetrically, the majority of minerals are either anhydrous or weakly hydroxyl-bearing.

Over 72 species of arsenic minerals and 48 species of zinc minerals are documented from FO, challenged perhaps only by Tsumeb. Many of these phases are found within the system $\text{CaO-ZnO-MnO-SiO}_2\text{-As}_2\text{O}_5\text{-H}_2\text{O}$. Most are hydroxyl-bearing (OH^-) compounds, that is phases which would crystallize in a basic environment. Such an environment is easy to provide. Calcite, CaCO_3 , is the major component of the FM and it is constituted of a strong base (CaO) and a weak acid (CO_2). A pH range greater than 7 (neutrality) would be expected from low temperature ($<300^\circ\text{C}$) reactions and fluid exchange with the marble. Native lead, Pb, and pyrochroite, $\text{Mn}(\text{OH})_2$, would be

stable in even more basic regimes. With “peculiar” primary minerals and with hydrothermal refluxing and diminishing temperature, the enormous number of FO species is not at all surprising. Basic environments are known to promote species diversity (consider the basic rocks nepheline syenites, tinguaite, foyaites, jacupirangites, carbonatites, etc. and the very basic species natrophosphate, $\text{Na}_7\text{F}(\text{PO}_4)_2(\text{H}_2\text{O})_{18}$ from the Kola Peninsula, Russia, a region which includes over 500 species of minerals!). How basic can you get? Acid environments, on the other hand, break chemical bonds, and oxidize cations. A radically different chemical crystallography emerges where the tightly-knit basic structures surrender to open loosely-knit structures held together by hydrogen bonds in the acid paragenetic setting. The myriad minerals containing As and Pb at FO comprise volumetrically a trivial to trace proportion of the FO ore bodies. What I will talk about are the *crème de la crème* of FO exotica, and how their crystal structures respond to the environment.

After this introduction, the next topic I will discuss is closest-packing. This topic is exceedingly difficult to present, so I will invite the reader to explore it directly. It is at once one of the easiest and the most esoteric of all scientific knowledge. Concepts in closest-packing are as important for mineralogists (though few of them get it right) as for mathematicians, and astrophysicists who study black holes. As you may be bored stiff by now, I'll whet your appetite with names like hemimorphite, hodgkinsonite, holdenite, gerstmannite, clinohedrite, junitoite, kolicite, franklinfurnaceite, pyrochroite, zincite. What do they all have in common? They are all closest-packed structures! And there are many more.

Before I get into the epistemology of closest-packing, allow me a more reflective approach. Nature, and our perception of Her, is based on a fundamental truth: economy. Our perception may screw it up, but Nature is incredibly economical. No waste. Darwin has shown us that for all living things, only the most economical survive *with respect to their environment*. In fact, parsimony minimizes the energy-driving entropy of disorder.

What we need is a Darwin of mineralogy. The ‘bloody tooth and bloody claw’ is seen in the paragenesis. Minerals are devastated (or created) by changes in fluid composition, pressure, temperature, oxygen fugacity, pH, oxidation potential, etc.. FO aren't really that peculiar. I still believe Langban has many more species. Almost no research is, however, going on in that incredible assemblage. But FO has been pored and picked over without relief. By the way, the Langban host rock is a marble. That is one reason why Langban and FO have much in common. But their ores are different. The major ore at Langban was braunite, $\text{Mn}^{2+}\text{Mn}_6^{3+}\text{SiO}_{12}$. It has yet to be found at FO.

What really excites me are the plethora of closest-packed structures found as crack minerals and listed in Table 1. Such information can only come from crystal structure analysis, that technology which few mineralogists today seem to comprehend. Representation of that structure is another matter: most fail miserably. People often ask me how I come up with these incredible representations and descriptions. I reply that the magic comes when I have plenty of Sebastian Bach in the background. Closest-packing, densest-packing — all variations on the same

theme. Unfortunately, no one knows what densest-packing means for an array of ions of different sizes. This is the famous Dirichlet Domain or Voronoi Polyhedron problem, covered nicely in Okabe *et al.* (1992). So I stick to closest-packing of ions of the same kind, in particular oxide or O^{2-} .

What are the fundamental underlying concepts behind the awesome diversity of mineral species in the FO crack systems? These concepts must account not only for the diversity but also for the plethora of species peculiar to the FO deposits. Even more important is the peculiarity of their crystal structures. Many of the structure types have no counterpart elsewhere. The fundamental underlying *leitmotifs* are two rather abstract and beautiful concepts embracing all of mineralogy. One of these is the *concept of closest-packed spheres* (the chemical crystallographic principle) and the other is the *concept of oxidation potential (Eh) and acidity-basicity (pH)* — the thermochemical principle. I shall try to convince you that these two fundamental concepts are tightly interlocked, at least at somewhat shallow conditions (less than one Km in depth). The one is an inevitable result of the other. I propose two fundamental arguments: many of the crack minerals from calcite to franklinfurnaceite are crystallographically closest-packed (thus, the concept of closest-packing must be explained). Second, the crack minerals formed at extremely reducing conditions ($E_h \sim -1$ volt) in an extremely basic environment ($\text{pH} \sim 13$). These conditions are so alkaline that the early juices from which the crack minerals grew would probably dissolve a corpse within an hour!

CLOSEST-PACKING

The concept of crystallographic closest-packing is based on Nature's parsimony and economy. It is at once the most tangible and abstract of concepts. How many spheres of the same size can you fit in a given volume? Because oxide (O^{2-}) anions are much larger (radius of 1.40 Å) than the FO cations (0.2 Å for Si^{4+} to 1.0 Å for Ca^{2+}), the anions take up the volume while the cations occur in the anion interstices in closest packing (see Figure 1). The famous closest-packing problem had its origins nearly 400 years ago in 1611 from the German astronomer-mathematician Johannes Kepler (“the Harmony of the Spheres”). Kepler was intrigued by the packing of the spherical “loculi” in pomegranates. Although he didn't prove it, he concluded that the most economical or parsimonious packing was a face-centered cubic arrangement, e.g. one of the closest-packings. The pomegranate “loculi” are equivalent to a pyramid of stacked pool balls. The *efficiency* of packing V_E , that is the closest-packing volume of spheres divided by the total volume, includes some irrational numbers, $V_E = \pi / 3\sqrt{2} = 0.7406$. In principle, this is the densest arrangement, where 74%+ of space is occupied by equivalent spheres, say O^{2-} . However, this famous problem was not proved until Prof. Wu-Yi Hsiang recently came up with an enormous proof, over 100 pages in length (Cipra, 1991)! This awesome proof, one of the largest in the history of mathematics, is not yet published as critical eyes pore over it. Word has it that a few flaws have been detected but that none of them is, as yet, fatal to the proof.

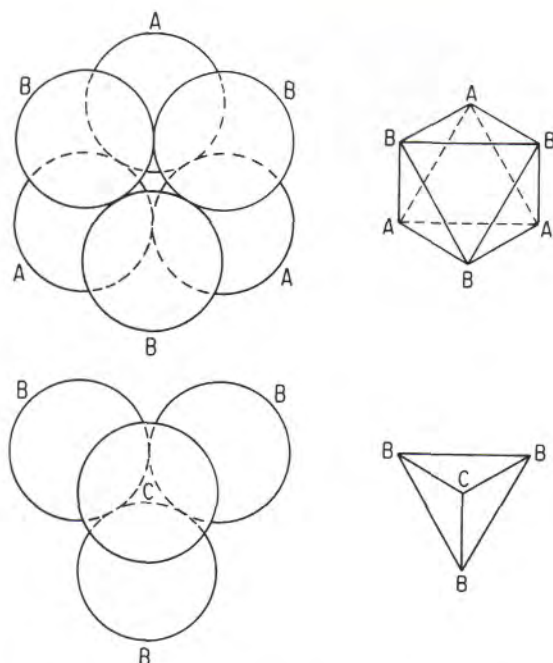


Figure 1. Octahedral and tetrahedral components of closest-packing. The sphere representation (left) and polyhedral representation (right) of the ideal octahedron (above) and tetrahedron (below) are featured. Note the sequence A-B-C.

Consider Figure 1, the two fundamental parts — the octahedron and the tetrahedron — which make up the polyhedral arrangements in closest-packings. We can represent closest-packing by either arrangements of spheres or linkages of polyhedra. To prove that octahedra and tetrahedra of the analogous polyhedral representation make up closest-packing is tedious but not difficult. The octahedral arrangement of spheres (upper left) has two layers: A (below) and B (above). Note the empty void in the center. This is where the small octahedrally coordinated cation goes. For convenience, the coordination polyhedron is constructed by joining the centers of nearest spheres together, creating the octahedron (upper right). The centroids of the spheres on the left have the same distances to each other as the polyhedral edges on the right in Figure 1. Note that the integers $N_0 =$ vertices, $N_1 =$ edges, $N_2 =$ faces of the octahedron. The octahedron is one of the Platonic solids, that is all vertices are equivalent, all edges are equivalent, and all faces are equivalent. Note that there are $N_0 = 6$, $N_1 = 12$, $N_2 = 8$ for the octahedron (count them)! There is the important Euler characteristic: $N_0 - N_1 + N_2 = 2$. This applies to all maps on the surface of a sphere, that is all convex polyhedra. For the *octahedron* $6 - 12 + 8 = 2$. Could we have $8 - 12 + 6$ which must give the same value (we only interchanged vertices and faces, both of which themselves are positive values)? The object has 8 vertices, 12 edges, and 6 faces. This is the *cube*. Cubic coordination occurs for cations of large radii coordinated by oxide in crystals such as Na^+ , K^+ , Sr^{2+} , Ba^{2+} , REE^{3+} . The cube, however, usually doesn't exist in closest-packed systems, but the local $\cdot C A B C \cdot$ packing geometry can be seen along the [111] direction of body diagonal of the cube. The switching of N_0 and N_2 leads to an important property called *duality*. The cube is the dual of the octahedron and vice versa:

vertices of one correspond to faces of the other. Draw a cube. Take the midpoints of each of the cube's faces. Connect these midpoints together. You get the octahedron. In Figure 1 (bottom, left and right) we have the *tetrahedron*. Here $N_0 = 4$, $N_1 = 6$, $N_2 = 4$ or $N_0 - N_1 + N_2 = 4 - 6 + 4 = 2$. The tetrahedron is a Platonic solid. The dual of a tetrahedron is a tetrahedron (cahnite twins in this fashion). For completeness, a medium-sized proof will demonstrate that there are only five Platonic solids where equivalence (homogeneity) reigns. The remaining two are the icosahedron and the pentagonal dodecahedron which are duals of each other. Strictly speaking they cannot be found comprising the cells of crystals because 5-fold symmetry is forbidden in periodic homogeneous lattices (another simple proof: it takes up two lines but gets wordy in the introduction!).

There are three ways to arrange closest-packed layers with minimum distance h between the layers and this is shown in Figure 2. Label these layers of closest-packed spheres as A, or B, or C. Note that the minimum distances within layers are

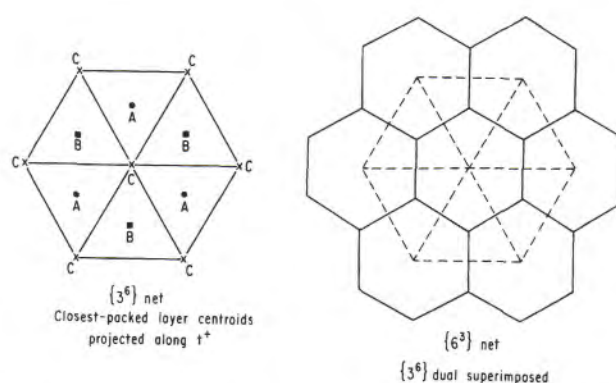


Figure 2. Representation of closest-packed layers as nets $\{3^6\}$ and the dual $\{6^3\}$, which are projected along t^* . Note correspondence to Figure 1. Duality is expressed in the right figure.

A - A = B - B = C - C. Each of them makes up a $\{3^6\}$ net, that is 3 \Rightarrow triangle (order) and 6 \Rightarrow number of triangles at a vertex or *node* (connectivity). Note that the dual of $\{3^6\}$ implies $\{6^3\}$ or the *hexagonal net*, see the construction on the right. Ah! You have made an insight: everything reduces to *equivalence*, the basis of an enormous mathematical discipline called *group theory*. One application of group theory is the science of *crystallography*. There are only three regular homogeneous nets (nets whose polygons are all equivalent and all connectivities the same): $\{3^6\}$, $\{6^3\}$, and $\{4^4\}$, the braces denoting regularity. The last is the square net. The dual of a triangular net is an hexagonal net, but the dual of a square net is a square net just as the dual of a tetrahedron is a tetrahedron as we just saw. Net and dual are shown in Figure 2. Basically, the construction of closest-packed structures proceeds from the triangular net. Figures 1 and 2 are here cut-outs over portions of the infinitely extending triangular net. As there are at most a sequence of three layers A, B, and C or (ABC) as in the *cubic* sequence along [111] of the cube (we are back to Kepler again!), it seems the problem is simple. It isn't. We could have the sequence (ABA) or the *hexagonal* sequence. We cannot use (AA),

(BB), or (CC) because such sequences are on top of each other and h is not minimized. Use the condensed nomenclature (ABC) = c and (ABA) = h . Each condensed symbol corresponds to a layer and it expresses adjacency. Note for c , the symbols adjacent to B are different. For h , the symbols adjacent to B are the same. For pure sequences, we have

... A B C A B C A B C ... or cubic closest-packing
 | | | | | | |
 ... c c c c c c c c ... or ccc, a three-layer repeat

and

... A B A B A B A B A B ... or hexagonal closest-packing
 | | | | | | | |
 ... h h h h h h h h ... or hh, a two-layer repeat

The repeated dots denote a repeating string of symbols. There are infinitely many closest-packed sequences, a simple and famous one being

... A B A C A B A C ... = chch or ch.
 | | | | | | |
 ... h c h c h c ...

This is the double hexagonal closest-packing or the topaz closest-packing, so called because the oxide anions in the topaz crystal have this kind of sequence. Some crystals are very complex, such as Mcgovernite which probably has 84 layers in its repeat! (See Moore and Araki, 1978). The Mcgovernite sequence (which has $c = 203 \text{ \AA}$, $203 \text{ \AA} / 84 = h = 2.42 \text{ \AA}$ or the layer separation) has practically the same layer separation as that for tephroite, $h = 2.44 \text{ \AA}$, which has the olivine or hexagonal closest-packed structure. Mcgovernite remains a structural monstrosity, an as yet unsolved DNA-like problem.

Oddly, many of the closest-packed structures of the peculiar FO crack minerals were not recognized as such by the initial investigators of these crystal structures. This held back progress in understanding their fundamental principles such as paragenesis, for decades. Part of this is due to the fundamental difficulty of recognizing closest-packing in maps of crystal structures. What if t^* , the vector normal to the closest-packed layers, is in a direction involving more than one of the selected crystallographic axes? This is common. The key is to find t^* . Once obtained, matrix theory does the job. It was the most time-consuming part of the study.

One little comment. Trigonometric relationships in closest-packed structures constitute a pleasant pastime. The most sensible approach is to construct the perfect model. In this model, all edge lengths are equal. Call this l .

Thus $h = \sqrt{2} / \sqrt{3} l$, h being parallel to the t^* vector normal to the closest-packed layers. The volumes of octahedron and tetrahedron can be computed in terms of l (derive them!).

Let's start with a layer of closest-packed spheres. Go out to the Five and Dime and purchase about 20 ping-pong balls of the same size. In Figure 1, locate the centroids (centers) of the spheres in a plane. Make a sheet of spheres. The net is $\{3^6\}$, that is six triangles (3) with six of their vertices meeting at a common point. Or you can use the dual $\{6^3\}$. Here, one sphere is surrounded by six other spheres of $\{6^3\}$, all kissing (touching the central sphere). Assuming you have enough spheres, make several sheets with about ten spheres in a sheet. When assembled and assuming you got it right, tickle and glue the spheres together where they kiss with a dab of Duco[®] cement.

Now place a second layer upon the first such that their thickness h is minimized. You will notice that the spheres of the second layer fit in the dimples of the first layer. Each sphere above will touch three spheres below. Look at the vacancies. About 74.06+% of space is filled by closest-packed spheres. Do you see tetrahedral and octahedral vacancies found in Figure 1?

Now put on the third layer. Aha! You discovered that there are two ways to do it (in one you can see octahedral holes all the way through). The other arrangement closes off the holes and you will see no light passing through. See Figure 2 for a projection of all three layers. Call the first layer A. Call the second layer B. Call the third layer which superimposes on the first and light comes through the A layer again. If light doesn't pass through, then call this layer C. But now you have ABA and ABC. Use shorthand ABA = h and ABC = c . The h is for a hexagonal layer and c is for a cubic layer. Note for the even B layer, adjacent odd layers are of the same kind for h and of a different kind for c .

You are now ready to construct closest-packed models of the gerstmannite, hodgkinsonite, and yeatmanite structures. It will be tougher than you think! Project along h or t^* , the vector of closest-packing. You will need little spheres of different colors to represent the positions of the octahedrally and tetrahedrally coordinated cations by the oxide anions. Of course, ion size is important. The Pauling radius for oxide, O^{2-} , is $1.4 \times 10^{-8} \text{ cm}$ or 1.40 \AA . Tables abound which give you sizes of ions. In fact, buy Pauling (1960), one of the greatest books on structure of this century. Radius ratio is a crude measure of ionic fitting.

Small cations usually tuck into the holes or voids left by the packed anions. If the radius of the cation (r_c) is divided by the radius of the anion (r_a), then $r_c/r_a = \sqrt{2} - 1 \sim 0.41$ gives an ideal octahedrally coordinated cation kissed by six anions at the vertices of an octahedron. Examples with O^{2-} include Mg^{2+} , Fe^{2+} , Fe^{3+} , Mn^{2+} , Zn^{2+} (acid), occasionally Ca^{2+} which is rather big ($r_c/r_a = 1.00/1.40 \sim 0.71$). If $r_c/r_a = \sqrt{3}/2 - 1 \sim 0.22$, then tetrahedral coordination of cation by oxide will occur. Here, four coordinating anions kiss the central cation. Examples are Si^{4+} , As^{5+} , S^{6+} , Zn^{2+} (basic), etc.

I stop here to state that crystallography is really applied group theory and matrix theory. You will need matrices to place many crystal structures into closest-packing representation. Unfortu-

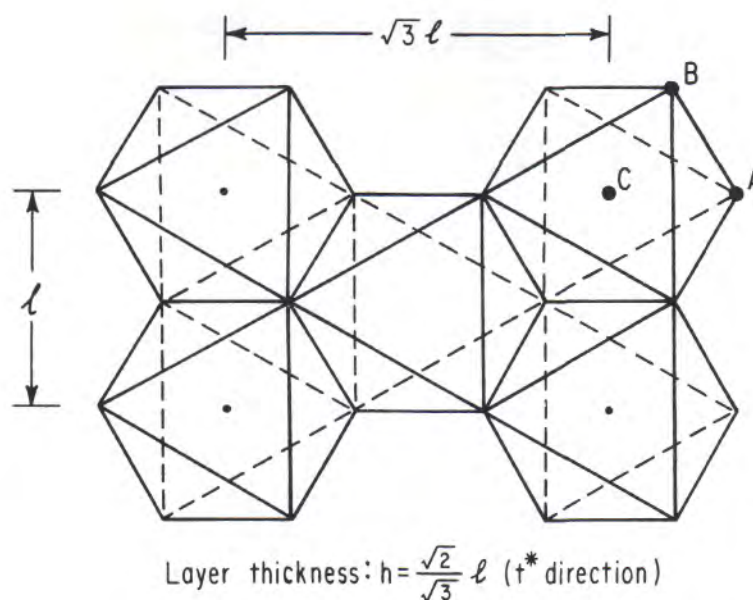


Figure 3. Orthohexagonal unit in cells of closest-packed structures. The edge length l and $\sqrt{3}l$ are perpendicular to each other. The layer thickness h is in the direction of t^* which is perpendicular to the closest-packed sheets.

nately, with the advent of home computers, people have become ignorant again, and the foundation subjects are all but forgotten. Palache didn't use group theory or matrix theory. What he used was an algorism (now embodied in software) to draw plans, clinographic and axonometric projections of crystals. An algorism is a recipe with a Ph.D.

How are closest-packed oxysalts checked beforehand? The ionic radius of 1.40 \AA for O^{2-} corresponds to a sphere with volume $V = 4/3 \pi r^3 = 11.50 \text{ \AA}^3$. The space it takes up in a crystal is $V_o = 1/0.7406 (11.50) = 15.52 \text{ \AA}^3$. Dividing unit cell volume by total oxygens gives V_o . Closest-packed oxysalt structures range from 15.0 \AA^3 to 22.0 \AA^3 . The octahedrally coordinated Mn^{2+} and tetrahedrally coordinated Zn^{2+} are fairly large ions for these coordinations. The V_o values for Table 1 hover around 21 \AA^3 . Most of the compounds include members of the Zn^{2+} , Mn^{2+} , and Ca^{2+} ions.

In ideal closest-packed structures, all atom centroids and the unit cell axes can be exactly specified using a set of algorisms to obtain the atom centroids and the bond distances. This perfect model is constructed from the perfect closest-packing (Figures 1-3) and the real crystal structure which determines atom centroids. Therefore, a difference, $\Delta(\text{\AA})$, can be taken between the real model and the ideal model. This difference has the real structure as the divisor and the atom coordinate pair difference as dividend. The quotient is $\Delta(\text{\AA})$. Usually, the real axes are chosen for the interatomic distance calculation between real and ideal structures. Values in $\Delta(\text{\AA})$ for Table 1 range from 0.0 to 0.8 \AA , with a mean of about 0.4 \AA . It is remarkable how closely the atom positions in the crystal track with the perfect model, the bulk of distortion in the crystal being a result of cation-cation repulsions. This I call the

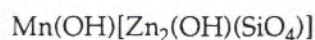
'cradle to grave' approach to analysis of a mineral's crystal structure.

HODGKINSONITE AS AN EXAMPLE

Hodgkinsonite is one of the more famous minerals from Franklin. The man honored was a miner and lover of Franklin minerals. It is reddish-brown to rich rose-pink in color with perfect basal cleavage. A crack mineral, it was once rather abundant in the Parker Shaft and north workings of the ore body. Broad pink cleavage surfaces contrasting with green willemite, occasional white barite, and the ubiquitous pyrochroite filled fractures cutting ore. Although once a common mineral in the Franklin workings, it has been noted from Sterling Hill only in moderate abundance, but nowhere else in the world.

There are many ways to express a mineral's formula. My tendency is to express a formula which optimizes the information in publication, especially the structure. The formula I prefer is $Mn(OH) [Zn_2(OH)(SiO_4)]$, a basic manganous zincosilicate. The formula suggests that some $(OH)^-$ is associated with the octahedrally coordinated Mn^{2+} ions, and some $(OH)^-$ associates with Zn^{2+} in the thick zincosilicate band or sheet. Parentheses serve as association. Brackets do the same but they usually denote the fundamental building block (f.b.b.) or underlying feature of the structure. The formula could be equally well written as $Mn(OH)_2 [Zn_2SiO_4]$ but this suggests one pyrochroite unit and one willemite unit, just fine if you are relating pyrochroite-willemite-hodgkinsonite thermochemically, but the structure speaks of a different bonding principle. The old dualistic formula, where everything is expressed as component oxides, would be $MnO \cdot 2ZnO \cdot SiO_2 \cdot H_2O$. Unfortunately, it says nothing

Hodgkinsonite



				(201/010/101)		cell
				$(\frac{1}{3} \ 0 \ \frac{1}{3} / 0 \ 1 \ 0 / \frac{1}{3} \ 0 \ \frac{2}{3})$		coordinate
Z	4	Z'	12		l	$\langle l \rangle$
a	8.171	a'	19.24	$6l$	3.21	18.66
b	5.316	b'	5.32	$\sqrt{3} \ l$	3.07	5.39
c	11.761 Å	c' (t*)	14.92 Å	$6\frac{\sqrt{2}}{\sqrt{3}} \ l$	3.04 Å	15.24 Å
β	95°15'	β'	90°48'	$h=2.49\text{Å}$	$\langle 3.11\text{Å} \rangle$	
$P2_1/a$		V'_E	21.2 Å ³	· h h h h h h ·		
Rentzeperis (1963), R = 0.07 / 946 F ₀						
Difference:	ΔMn	0.21		$\Delta \text{O(3)}$	0.59	
	$\Delta \text{Zn(1)}$	0.19		$\Delta \text{O(4)}$	0.96	
	$\Delta \text{Zn(2)}$	0.15		$\Delta \text{OH(5)}$	0.38	
	ΔSi	0.17		$\Delta \text{OH(6)}$	0.35 Å	
	$\Delta \text{O(1)}$	0.62		mean	0.39 Å	
	$\Delta \text{O(2)}$	0.28		range	0.15 - 0.96 Å	

Table 2. Hodgkinsonite crystallographic details.

See text for the relationship between this crystallographic cell and the cell transformed to conform with closest-packing. More details will be presented in the second part of this series.

about chemical bonding but is convenient for the chemical analyst. Mere atom ratios could be taken, i.e. $\text{H}_2\text{Mn}^{2+}\text{Zn}_2^{2+}\text{SiO}_6$. Again, not a hint of bonding chemistry is given.

Table 2 is an example of the central device I shall use in the second section. *Hodgkinsonite* heads up the table. Next is the formula. The matrix for the cell transformation (from old cell to new primed cell) is given in condensed form. Thus,

$$(201/010/101) \equiv \begin{pmatrix} 201 \\ 010 \\ 101 \end{pmatrix}$$

The cell transform is the fundamental step; the rest is recipe or mechanics. This matrix is often labeled **A**. The coordinate transform follows. This transform, labeled \mathbf{A}^{-1} , allows for the transformation of every atom coordinate from the old into the new primed cell. Note the new cell ($Z'=12$) has three times the contents of the old cell ($Z=4$). It belongs to one of an infinity of space groups, and usually destroys some of the equivalence classes (symmetry operations) of the old space group. Of the infinity of space groups, only 230 are irreducible. That is, they cannot be

reduced to simpler subgroups without destruction of their equivalence relationships. The 230 space groups are the ones you see in tables. Compound or reducible groups are, however, very handy in describing crystal structures according to some fundamental principle, in this case closest-packing. Technically speaking, the matrix \mathbf{A}^{-1} is obtained by first extracting the order of **A**. The adjoint of **A** is then obtained. The inverse, \mathbf{A}^{-1} , is then obtained from order and adjoint. Finally, the rows and columns are interchanged, giving the transpose and consequently \mathbf{A}^{-1} . All these manipulations can be conveniently found in Ayers (1962), a book which I used in high school. The matrices are the most crucial step in all the ensuing operations. Without a knowledge of matrices and groups, knowledge of a mineral structure is practically meaningless. Unfortunately, most mineralogists are more comfortable with knob-twisting and button-pushing than with fundamental concepts. And their knowledge of chemistry is abysmal!

The blocks which follow on the table are (left to right) the old cell and citation(s), the new cell including V_0 (pyrochroite, Mn(OH)_2 , has 22.8 Å³ per oxygen), and can be calculated from old

cell or new cell. It is the unit cell volume divided by the total oxygens in it. For Pauling radius $r_o = 1.40 \text{ \AA}$, $V_o = 15.5 \text{ \AA}^3$. Clearly, bigger cations (such as Mn^{2+} , Zn^{2+}) lead to bigger numbers for packing efficiency. Note t^* . This is the vector normal to the closest-packed layers. Because $l = \text{octahedral edge} = \text{tetrahedral edge} \approx \text{twice oxide radius}$, all transformed cell edges can be referred to l (*vide supra*). The three axes can be defined by integers

(n,m,p) : nl , $m\sqrt{3}l$, $p\frac{\sqrt{2}}{\sqrt{3}}l$ which are the edge direction, the edge normal, and the direction along t^* ; see Figure 3. The layer separation can be immediately extracted: it is $h \sim 2.5 \text{ \AA}$ for these structures. Finally, note that the transformed β' is close to 90° . In fact, the range for all these structures is $\beta' = 90^\circ \pm 4^\circ$, but the margins are too narrow to admit this proof. Deviations in crystals from orthogonality display the effect of cation-cation repulsions. Individual values for l are listed, and their mean in carats can be plugged into the primed cell relations in terms of l . This $\langle l \rangle$ gives an indication of the relative axial distortions due to cation-cation repulsion effects and so on, and can be compared with the axes of the real cell. They rarely deviate more than 5% from the transformed values. The structure, when projected along t^* , immediately gives the layer sequence. For hodgkinsonite, there are six layers in the cell repeat, in this case 'hhhhhh', or hexagonal closest-packing. I always label each layer according to h or c. The use of condensed nomenclature 'hh' is not advised because hodgkinsonite is *not* a two layer repeat structure (as pyrochroite is).

Finally, difference $\Delta(\text{\AA})$ is given. The transformed cell is chosen and an interatomic distance calculation is performed. The atom coordinates are those from A⁻¹ applied to the original data of Rentzeperis (1963). The *ideal* (perfect) coordinates can be calculated from any closest-packed system from several algorithms I derived. The close fit of all atom pairs speaks well of the power of difference for testing one's conclusions. If the structure report had an error or if the arrangement weren't closest-packed, nonsensical values would be obtained. The mean of 0.39 \AA for all unique non-H atoms is remarkable. The range $0.15 - 0.96 \text{ \AA}$ for hodgkinsonite is not bad either (the oxide radius is $r_o = 1.40 \text{ \AA}$). These are typical (though somewhat high) values for all the closest-packed Franklin phases I studied, which will appear in the future installment.

The entire Table 2 required a "Linus Pauling machine" or hand calculator, Burington (1940), and several homemade algorithms. Including a sketch along t^* , the entire table took 1/2 hour of labor — a tiny price to pay for such a wealth of valuable information.

In preparation for the next issue, I include the ideal structure representation of hodgkinsonite in Figure 4, its accompanying table in Table 2. The reader can pick at it and gear up for the many tables in the next issue. There, with figure and table, each species will be discussed in a terse overview of its structure and comments, if any, which may arise from peculiarities in the table. The structural part of this study is now concluded with a particularly interesting species.

One of the more remarkable crystal structures is found in franklinfurnaceite, $\text{Ca}_2\text{Mn}_3^{2+}\text{Mn}^{3+}\text{Fe}^{3+}(\text{OH})_8 [\text{Zn}_2\text{Si}_2\text{O}_{10}]$. It was first described by Dunn *et al.* (1987) from a Franklin crack mineral

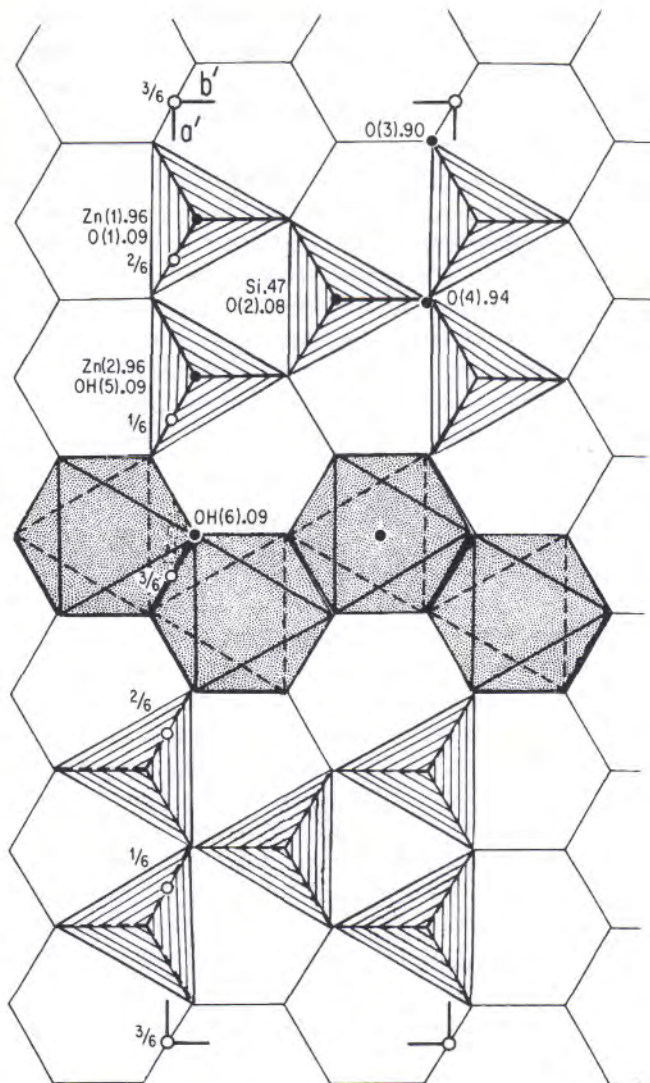


Figure 4. Hodgkinsonite ideal crystal structure projected on the $\{6^3\}$ net. The zincosilicate tetrahedra are ruled and the manganese oxyhydroxy edge-sharing octahedra are stippled. Note that the arrangement is one layer in thickness.

paragenesis which includes willemite, clinohedrite, hodgkinsonite, hetaerolite, and franklinite. In this association, franklinfurnaceite is one of the last minerals to form. Doubly interesting is its structure, reported in an extensive paper by Peacor *et al.* (1988). It is related to but distinct from the crystal structures of the chlorites. Of key importance is the fit between the octahedral and tetrahedral layers. A considerable rotation of the tetrahedron — owing mainly to the large ZnO_4 tetrahedra — leads to an arrangement which is nearly ideally closest-packed, so far unheard-of in chlorite structures. All anion slots are occupied and the packing sequence is "hccccch". Actually, this is not a 6-layer structure but a $3 \times 6 = 18$ -layer structure. You will see this if you transform the condensed nomenclature back to the (A,B,C) nomenclature. Normally, this is no problem because we usually begin with (A,B,C) placed on the structure projection along t^* in

the original map. Table 1 has several examples of condensed sequences which must be multiplied to get the repeat distance along t^* .

Several items make this structure even more interesting. Closest-packing is relatively rare in phyllosilicates. The unique chemistry of franklinfurnaceite (Ca^{2+} , Fe^{3+} , Mn^{2+} , Mn^{3+} , Zn^{2+} , Si^{4+} cations) coupled with the closest-packing — associated clinohedrite, hodgkinsonite, hetaerolite, franklinite and calcite are closest-packed — make this late formed mineral especially attractive. One wonders how many novel closest-packed oxysalts occur in a similar paragenesis but are overlooked because of their mimetic appearance to some common species. Franklinfurnaceite is a particularly good example of the apparent relationship between closest-packing and very basic environment for formation.

OXIDATION-REDUCTION

The paragenesis is about the most fundamental knowledge we can glean of a mineral's occurrence. The term means "beside the origin" or "next to the origin". This is because our first observation presents neither crystal structure nor optical characters but associations of the phase with other phases in time and space. Usually, the crystallizing fluid is long gone and we have been forced since the beginning of mineralogy to list these associated solid phases including amorphous material (gel). In principle, the sequence of phases can be worked out in time (temporally) and in space (through associations). From study of a suite of such samples, a paragenetic diagram, usually in coordinates of *species-relative time*, can be worked out. Note that absolute time is usually not known. Such time is usually measured with a clock, e.g. an unstable isotope or isotopes with known decay rate(s).

Unfortunately, such construction of a paragenetic diagram or tree assumes that the phases crystallized sequentially, but says nothing about absolute time interval. Even assuming the absence of replacement phases, we still have a problem. In such an interval it is possible, maybe even likely, that the coexisting fluid from which the crystals grew, may have experienced pronounced changes in important fluid parameters such as oxygen fugacity, oxidation potential, and pH. Because phase A sits upon phase B, it does not mean that A and B crystallized sequentially from the *same* fluid, that is B having crystallized first, then A crystallized upon it. Providing fluid still has access, it is possible that the crystallizing of A and B could be separated in time by hundreds of million of years. After all, crystal B is a good substrate for a later growth of A. The earliest crystal possesses an organized surface, upon which a later crystal could find it energetically more favorable than growing directly from the fluid. Palache (1935) lists and discusses many examples of paragenesis at FO.

Mineralogists have expended great energy in deciphering species sequences in simple and complex systems. But short of determination by isotope geochemistry the absolute age dates for each of the crystallizing phases in the sequence, there is no easy way to sequence a paragenetic suite with respect to absolute time. Most paragenetic diagrams have many connections which, stated or tacit, are based on a lot of assumptions. To circumvent this problem, appeal must be made to some general experimental

technique. This is solution thermochemistry. Even here, knowledge of mineral associations is absolutely necessary and this is gleaned largely from samples. Certain phases may recur over and over again in different paragenetic settings and in chemically different systems. Willemite and calcite are good examples of this. If a mineral's thermochemical stability is fairly well-known for a particular paragenesis, it may be considered an indicator mineral. It may place reasonable limits (such as oxygen fugacity, oxidation potential, pH) on the phases which coexist with it, even though thermochemical parameters may not be known for the associated minerals.

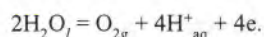
The indicator phase in question at FO is pyrochroite, $\text{Mn}(\text{OH})_2$. This mineral occurs in association with many of the "peculiar" FO crack minerals. Unfortunately, because of its relatively ubiquitous occurrence at FO, pyrochroite has been, if anything, underestimated in lists of phases where it is associated with these exotic minerals.

Pyrochroite was chosen because the phase has a simple composition and because it appears to occur at extremely limited conditions of formation. Garrels and Christ (1990), the reference which I use in this section and from which most of the equations are taken, and an excellent step-by-step survey of solution chemistry, are insistent upon this one (p. 241): "No wonder the hydroxide pyrochroite is an extremely rare mineral; it requires alkaline reducing conditions and the practical absence of CO_2 ." In fact, pyrochroite's field of stability has a centroid (see p. 242) at an oxidation potential Eh about -0.4 volts and pH almost 13. This is an exceedingly reducing basic brine.

Such exceedingly basic and very reducing solutions are rare on Earth's crust. Things tend to be more oxidizing. All occurrences are in carbonates such as calcite, dolomite, and rhodochrosite. If the very basic solutions came later, it does not necessarily follow that much carbonate was in solution coexisting with the reduced cations. Pyrochroite occurrences include FO; the Chicagon Mine, near Iron River, Iron County, Upper Peninsula, Michigan (here the unique seamanite, $\text{Mn}_3(\text{OH})_2(\text{PO}_4)\text{B}(\text{OH})_4$, occurred); Bergslagen district in Sweden; Gonzen, Switzerland; Noda Tamagawa Mine and many others in Iwate Prefecture, Japan; also several other small occurrences throughout the world, especially with carbonates which crystallized earlier. At the conclusion of this section, I will offer a provisional mechanism for the formation of such basic fluids.

The oxidation potential referred to the standard hydrogen electrode is written Eh, expressed in volts. The more positive and higher the Eh, the more oxidizing the environment. Later we will see that the mnemonic "acid-oxidation, base-reduction" has a real foundation.

To refer the reader to Garrels and Christ (1990) alone is unfair. Thermochemical relations, of which potentially very many parameters are involved, must be precisely specified. In any reaction, there is an equation, for example:



On the left, it reads two moles of liquid water. On the right, molecular oxygen gas, four hydrogen ions in the aqueous liquid, and four electrons. The system is balanced: four hydrogen ions (+)

and four electrons (-) balance, with neutral chemical species remaining. In the relations that follow, activity (concentration) of pure liquid water and partial pressure of oxygen gas are taken as unity. We will express this equation as a *half-reaction*, that is reduced state = oxidized state + ne, for example $Mn^{2+} = Mn^{3+} + e$, or manganous ion (pink) goes to manganic ion (red) plus one electron.

Consider a half-reaction involving n electrons $aA + bB = cC + dD + ne$. From the fundamental Law of Mass Action, the thermodynamic equilibrium constant for fixed temperature (T, here 25° C) is: $K = [C]^c [D]^d / [A]^a [B]^b$, concentrations in brackets.

The standard half-cell potential (E° , in volts) and standard hydrogen electrode half-cell potential (E_h , in volts) can be related, viz.:

$$E_h = E^\circ + \frac{RT}{nF} \ln K.$$

In thermochemical reactions, the proper expression of units can become exceedingly complex. On p. 17, Garrels and Christ (1990) write out such a relationship, which I present in similar form. Note the constant R, the gas constant; and F, Faraday's constant. Temperature is expressed on the absolute Kelvin scale. At 25° C, $K = (273.15 + 25) = 298.15$ K. Heat is measured in calories (cal.). At 25° C (298.15K), the constants are:

$$\frac{RT}{F} = 2.303 [1.9873 \text{ cal/deg } (298.15 \text{ K})] / [23062.3 \text{ cal/volt gm equiv.}] = 0.0592.$$

Included is the conversion from the natural logarithm to the Briggsian (base ten) logarithm, that is $\ln x = 2.303 \log x$. Also note that algorithm and logarithm have very different meanings, the first named after an ancient Arabic mathematician. The units for 0.0592 are rarely expressed; they are **volt equivalent/deg mole**. This value is temperature dependent, the value here expressed for 25° C (298.15 K).

From the previous relationships, $E_h = E^\circ + 0.0592/n \log K$. The equation for the upper limit of water stability is (see Figure 5): $2H_2O(l) = O_{2g} + 4H^+_{aq} + 4e$, which was earlier discussed. The relation is: $E_h = E^\circ + 0.0592/4 \log [H^+]^4$. Here n = 4 or four electrons, and H_2O and O_2 are each set at unity. By definition, set - pH = log [H+]. Then:

$$E_h = E^\circ - 0.0592 \text{ pH}.$$

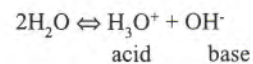
This equation links the oxidation potential (E_h), with respect to the standard hydrogen electrode, to the standard potential (E°), and to the pH, or negative logarithm of the hydrogen ion concentration. Such a diagram, with E_h on the ordinate and pH on the abscissa, can be mapped providing E° is known. Values for E° can be derived from the standard free energies of formation in Appendix 2 of Garrels and Christ (1990). These values were empirically determined and sources are given.

An outline of the relation at 25° C between E_h and pH for water appears in Figure 5. At pH = 0, the boundary between H_2O and O_2 occurs at 1.23 volts. At pH = 14, it is 0.401 volts. The lower

boundary at pH = 0 at 0.0 volts (set by the hydrogen electrode), terminates at -0.829 volts for pH = 14 and demarcates the field between water (H_2O) and hydrogen (H_2). Between these two boundaries, water is stable. Above the upper boundary, the system is oxidizing (free oxygen) and below the lower boundary the system is reducing (free hydrogen). The geochemically typical fields of phase stability occur between these two boundaries in the field of water, and most diagrams are constructed within this water field. It should be remarked that the upper left corner of Figure 5 is the acid-oxidizing environment while the lower right corner is the base-reducing environment.

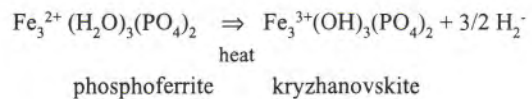
THOUGHTS ON PARAGENESIS

The question immediately arises how such basic and reducing conditions for pyrochroite can appear in nature. A mechanism should be found which, in related carbonate environments, leads to such extreme conditions. One simple equation immediately comes to mind, the acid-base equation, viz.:



To create this spontaneously and segregate H_3O^+ (acid cation) and OH^- (base anion) would require a considerable amount of energy. We have to look for a reasonable mechanism. Hopefully, this mechanism would be based on a realistic model. If, in the acid-base equation, a means were found to remove from the closed system either H_3O^+ or OH^- , concentration with time would lead to a very acid or basic environment. Unfortunately, the mechanism I propose is based on heat as the means of driving the reaction; but a further demonstration is required.

The fundamental question is how are such exceedingly basic (pH ~ 13) and reducing ($E_h \sim -0.5V$) conditions attained. Despite the great importance of redox reactions in Earth's crust and a large experimental literature on the subject, mechanistic approaches which address just this problem are but few. In a series of papers on $Fe^{2+} \Rightarrow Fe^{3+} + e$ reactions in crystals, Moore *et al.* (1980) subsequently proposed an intracrystalline auto-oxidation-reduction model. The transition metal was oxidized, its valence state was changed but there was *no* evidence of structural destruction in crystals of certain species. The most telling example was phosphoferrite, a mineral from granite pegmatites:



Rather detailed crystal structure analyses on synthetic hydrothermally grown pale green phosphoferrite and its later produced oxidation product of red-brown kryzhanovskite were undertaken on the same crystal by Moore and Araki (1976). To achieve this, a large diffraction sphere of data was collected from phosphoferrite. After the experiment, the crystal was removed and heated in air at 180° C in a muffle furnace for 48 hours. A similar data set was collected on the red oxidized kryzhanovskite. Although

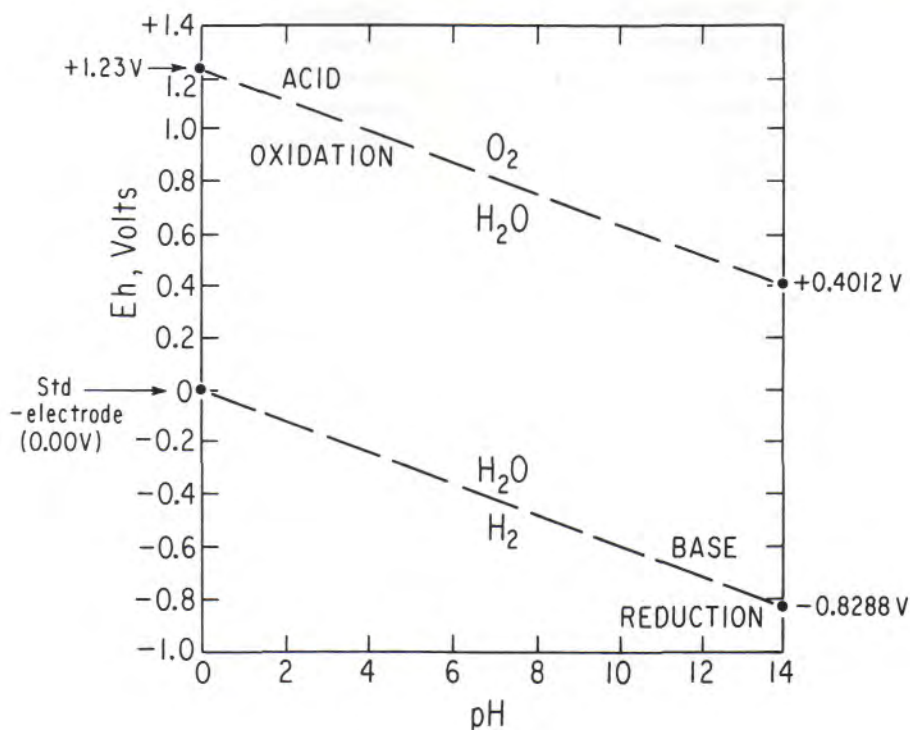


Figure 5. Oxidation-reduction diagram of water. The Eh is in volts, and pH is the negative logarithm of the hydrogen ion concentration. Note free oxygen above, free hydrogen below. Most Eh-pH diagrams are within this field.

kryzhanovskite had a smaller unit cell than phosphoferrite, half the hydrogen atoms were missing in this oxidation product.

Evidence supported the same space group for the two end-members. For these compounds, the crystal structures revealed that the ferrous (and ferric) members had two Fe^{2+} (Fe^{3+}) bonded to each water (hydroxyl) molecule. Thus, the oxygen atom (of the water molecule) has two bonds from Fe^{2+} and two short bonds from the two hydrogen atoms, giving an electrostatically favorable arrangement. Three Fe^{2+} bonded to a water molecule are electrostatically not favored, hence have not been seen. Rather, they are attached to a hydroxyl (OH^-) group. One Fe^{2+} bonded to a water molecule is very common and is seen in many crystals. However, when these crystals are heated in air, they break down to amorphous material.

Here is a possible way to split off hydrogen, remove it as a gas, and create ever increasing amount of (OH^-) base with time. It only requires moderate temperatures ($\sim 200^\circ \text{C}$). Unfortunately; only half of the experiment has been done. The earlier experiment was done in the presence of the atmosphere. It remains to repeat the experiment *in vacuo* (absence of oxygen). Such an experiment, if it succeeds, would state that the reaction and the splitting of hydrogen are indeed intracrystalline. The number of FO minerals at low temperature which have two M^{2+} and two H^+ cations bonded to an oxide anion is not known. A phase which such structure should be common and fit in the FO paragenetic scheme.

More work needs to be done. The pyrochroite paragenesis is incompletely described. How it occurs, with which species it

occurs, and just how abundant it is, are important questions to answer. Closest-packing does also occur in other crystal structures beyond Table 1 from FO. This principle is easy to overlook.

Eh-pH relations within the FO paragenesis are very poorly understood. Approximate calculations are possible through Appendix 2 in Garrels and Christ (1990) and, because the crystals are based on principles of closest-packing, the fields of stability thus derived may have some meaning. Presently, more immediate problems are in store, in particular the natural paragenesis.

But most impressive is the list of closest-packed structures in Table 1. World-wide, this FO list may be without equal, with Langban as a possible second. Of the chemically related complex basic and aquated transition metal phosphates from the Palermo Mine, there are 62 hydrothermal phases and the structures are known for nearly all of them. Not one possesses a structure based on the closest-packing principles. These phases certainly grew under more acidic conditions than the crack phases at FO. Synthetic crystals which were grown in decidedly more acidic conditions ($\text{pH} < 3$) tend to possess corner-linked octahedral-tetrahedral open framework structures. Synthetic, $\text{Fe}_3^{3+}(\text{H}_2\text{O})_3[\text{PO}_3\text{OH}]_3[\text{PO}_2(\text{OH})_2]_3 \cdot 3\text{H}_2\text{O}$, is a fine example, see Moore and Araki (1979). Such structures are far removed from the closest-packed systems, but are markedly open, akin to the very open corner-linked tetrahedral zeolite structures.

These observations are exciting. It is expected that very complex low temperature mineral assemblages will reveal to us the link between crystal structure and mineral paragenesis.

ACKNOWLEDGMENTS

Interested individuals who have been following the progress of chemical crystallography (crystal structures) from 1960 onward, will note that a great activity in crystal analysis occurred roughly between 1960 and 1985, followed by a period of relative quietude. I was funded during this period by the National Science Foundation. It was a period of magnificent construction of a data base. In this study I acknowledge NSF EAR-90-05742 for support of what I hope is the *synthetic* part, that is to say putting these structures unraveled by myself and many other workers to good use in a primitive but bold attempt to relate crystal structure to mineral paragenesis.

Especial thanks is directed to Mr. John L. Baum, a keeper of the Franklin flame, and the man who may have started it all for me back in 1953.

REFERENCES

- Ayers Jr., F. (1962) Theory and Problems of Matrices. Schaum's Outline Series, McGraw-Hill, New York, 219 pp.
- Burington, R.S. (1940) Handbook of Mathematical Tables and Formulas, 2nd. ed. Handbook Publishers Inc., Sandusky, Ohio, 275 pp.
- Cipra, B. (1991) Music of the spheres. *Science* **251**, p.1028.
- Dunn, P.J., Peacor, D.R., Ramik, R.A., Su, S.-C., Rouse, R.C. (1987) Franklinfurnaceite, a $\text{Ca-Fe}^{3+}\text{-Mn}^{3+}\text{-Mn}^{2+}$ zincosilicate isotopic with chlorite, from Franklin, New Jersey. *American Mineralogist* **72**, 812-815.
- Garrels, R.M., and Christ, C.L. (1990) Solutions, Minerals, and Equilibria. Jones and Bartlett, Boston, 450 pp.
- Moore, P.B., and Araki, T. (1976) A mixed-valence solid solution series: crystal structures of phosphoferrite and kryzhanovskite. *Inorganic Chemistry* **15**, 316-321.
- Moore, P.B., and Araki, T. (1978) Hematolite, a complex dense-packed sheet structure. *American Mineralogist* **63**, 150-159.
- Moore, P.B., and Araki, T. (1979) Crystal structure of synthetic $(\text{NH}_4)_3\text{H}_3\text{Fe}^{3+}(\text{PO}_4)_6 \cdot 6\text{H}_2\text{O}$. *American Mineralogist* **64**, 587-592.
- Moore, P.B., Araki, T., Kampf, A.R. (1980) Nomenclature of the phosphoferrite structure type: refinements of landesite and kryzhanovskite. *Mineralogical Magazine* **43**, 789-795.
- Okabe, A., Boots, B., Sugihara, K. (1992) Spatial Tessellations: Concepts and Applications of Voronoi Diagrams. John Wiley, New York, 532 pp.
- Palache, C. (1935) The Minerals of Franklin and Sterling Hill, Sussex County, New Jersey. U.S.G.S. Professional Paper 180, Washington, 135 pp.
- Pauling, L. (1960) The Nature of the Chemical Bond. Cornell University Press, Ithaca, N.Y., 644 pp.
- Peacor, D.R., Rouse, R.C., Bailey, S.W. (1988) Crystal structure of franklinfurnaceite: a trioctahedral zincosilicate intermediate between chlorite and mica. *American Mineralogist* **73**, 876-887.
- Rentzeperis, P.J. (1963) The crystal structure of hodgkinsonite, $\text{Zn}_2\text{Mn}[(\text{OH})_2\text{SiO}_4]$. *Zeitschrift für Kristallographie* **119**, 117-138.



SPRING 1994 FOMS MINERAL SWAP - AND - SELL !!!

Can't tell you which weekend its going to be...
...but stay tuned...
Its bound to be bigger and better than ever ! Don't miss it !!



(watch for flyer or turn up at our first meeting)

GEOLOGY AND MINERALOGY

OF A

VEINLET ASSEMBLAGE ASSOCIATED WITH WOLLASTONITE-BEARING ROCKS, STERLING MINE, OGDENSBURG, NEW JERSEY

Robert E. Jenkins II
Mining Technology
E. I. DuPont de Nemours & Company
Wilmington, Delaware 19898

INTRODUCTION

Wollastonite-bearing rocks of the Sterling mine, Ogdensburg, New Jersey occur in two zones, one adjacent to the east branch of the west limb of the zinc deposit, the other proximal to the deposit's keel. The wollastonite-bearing rocks occur near the contact between the marble core of the deposit and the Pyroxene Zone of Metsger *et al.* (1958). This paper is concerned with the geology and mineralogy of an interesting veinlet assemblage which is associated with and perhaps in part derived from wollastonite-rich rocks near the keel on the mine's 700 Level. The veinlet assemblage includes the manganese epidote, piemontite, here reported from the Franklin-Sterling district for the first time. Piemontite is associated with barite, johnbaumite, rhodonite, and other species. This veinlet assemblage was apparently deposited by hydrothermal fluids, with component metals derived from local wall rocks, including the wollastonite-rich rocks, subsequent to opening of host fractures. The veinlet assemblage was exposed in the north wall of the 740 Crosscut, 700 Level, at approximate mine coordinates -1687, 739N, 980W. Coordinates follow the nomenclature of the New Jersey Zinc Company (NJZC), as described by Sanford (1992). About 25 kg of samples containing the veinlet assemblage were collected. The sampling site is now flooded.

GEOLOGY

The author never visited the veinlet assemblage locality. The descriptions of this section therefore derive from several sources. The observations of personnel of the Sterling Hill Mining Museum, and others who saw the site, were extremely helpful in producing an overview of the local geology of the veinlet assemblage area. All of these individuals are credited in the Acknowledgments section. The unpublished geologic maps of 500 and 700 Levels by Allan Pinger (1932), together with the author's unpublished maps of 340 Level and the 700 Crosscut, 600 Level (1991-92), were used to construct the general structural interpretation of the wollastonite-bearing rocks and the veinlet assemblage area. Figure 1 is a simplified geologic map of 700 Level, showing the area of the veinlet assemblage in relation to the zinc deposit and some of the rock types within the core of the orebody. The veinlet assemblage, together with the associated wollastonite-rich rocks, is exposed in the interior of the block of Calcsilicate Rock at right-center of the outlined Described Area. Rock units generalized under the heading Calcsilicate Rocks include the wollastonite-bearing rock; pyroxene, pyroxene-feldspar, and pyroxene-garnet calcsilicates; and amphibolites and gneisses. The term Marble with Sparse Ore Minerals refers to impure marble containing sparse disseminated franklinite in addition to various silicate minerals, such as phlogopite, diopside, and willemite. Mineralogy and chemistry of some of the rock-forming minerals are

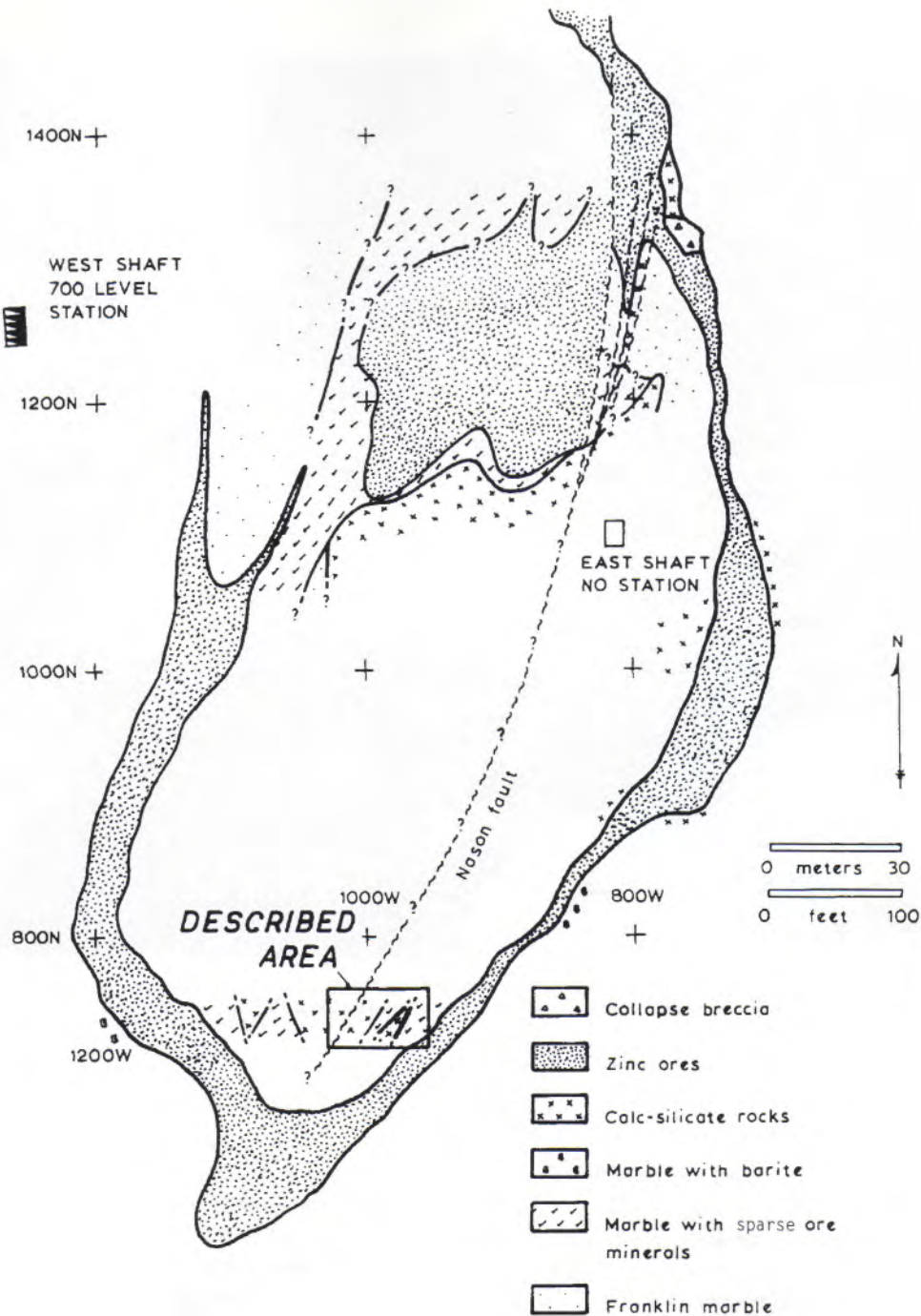


Figure 1. Simplified geologic map of 700 level, Sterling Mine, New Jersey, showing location of the veinlet assemblage and associated wollastonite-bearing rocks (based on geologic mapping by Allan Pinger, 1932; author's mapping in NE quadrant of mapped area, 1991; and New Jersey Zinc Company drift outline survey, 1979).

discussed in the succeeding section. Figures 2a,b illustrate the *in situ* occurrence of the veinlet assemblage and the wollastonite-bearing rocks on 700 Level. Calcite-apatite-wollastonite rock forms a small pod about 1x7 m, exposed in the north wall and near the floor of the crosscut, the long dimension of the pod oriented parallel to the floor. The pod is intricately folded (Figure 2b); but in general, it would appear to form part of the nose of a larger fold, plunging S, with foliation striking E-W and dipping S at the top of the pod, but striking N-S and dipping W on the west side, and

striking N-S but dipping in the opposite sense at the east edge. Foliation is defined by interlayered dark minerals, mostly hedenbergite, and by wollastonite. Bordering the pod is an irregular, discontinuous zone of hedenbergite-calcite-microcline rock (mapped Calcsilicate Rock of Figure 1) containing variable amounts of galena and sphalerite. Foliation is best developed in this zone near the pod of Wollastonite-rich rock, where microcline, calcite, and sulfides are most abundant and are interlayered with dark pyroxenes. Foliation is conformable with that in the

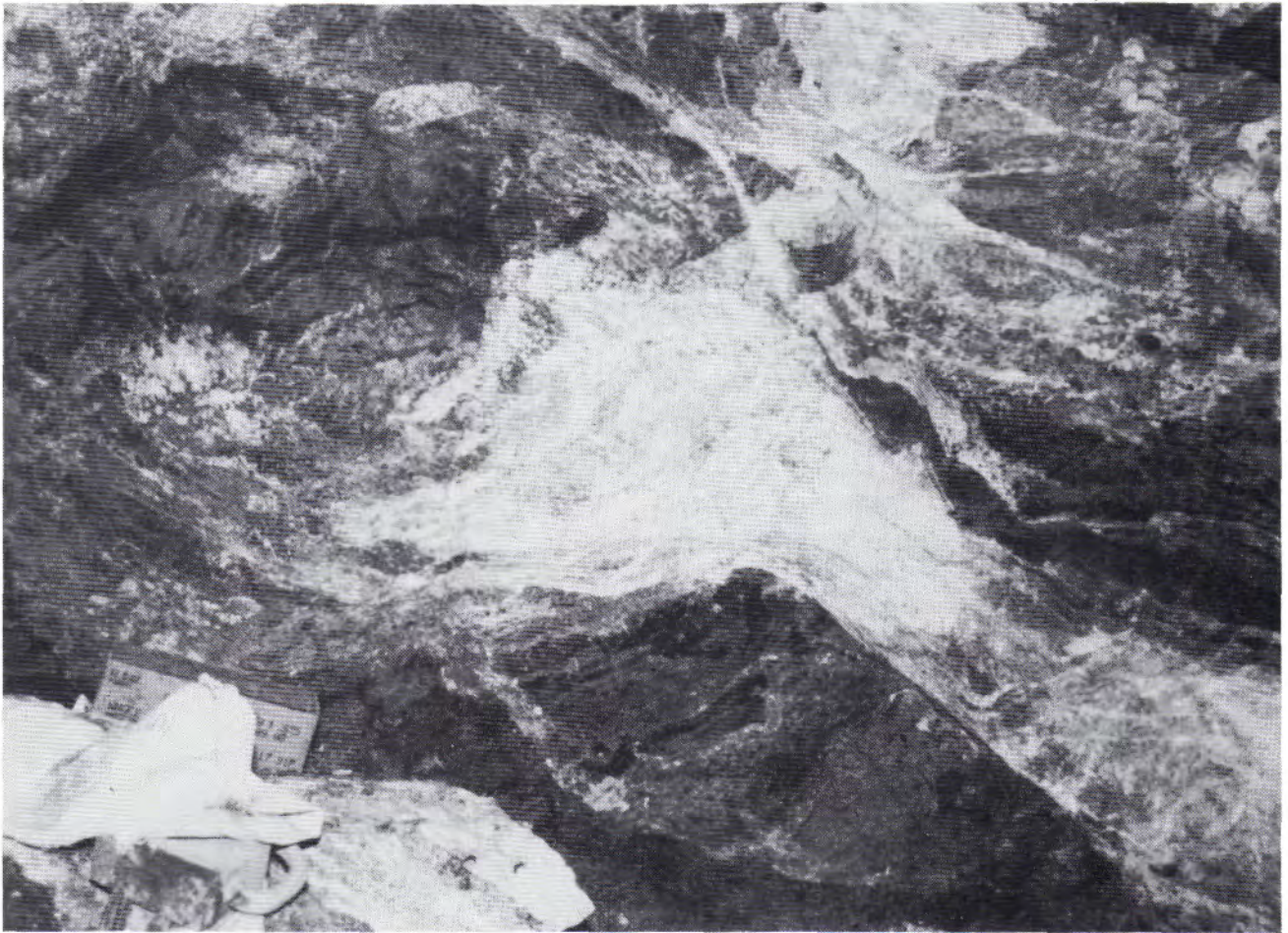


Figure 2a. West end of the pod of wollastonite-bearing rock, looking north, 740 crosscut, 700 level. Note contortion of wollastonite-bearing rock, and fingers of wollastonite-bearing rock extending into pyroxene calcisilicate rock. Field of view is about 0.7 m across; Steven Misiur photograph.

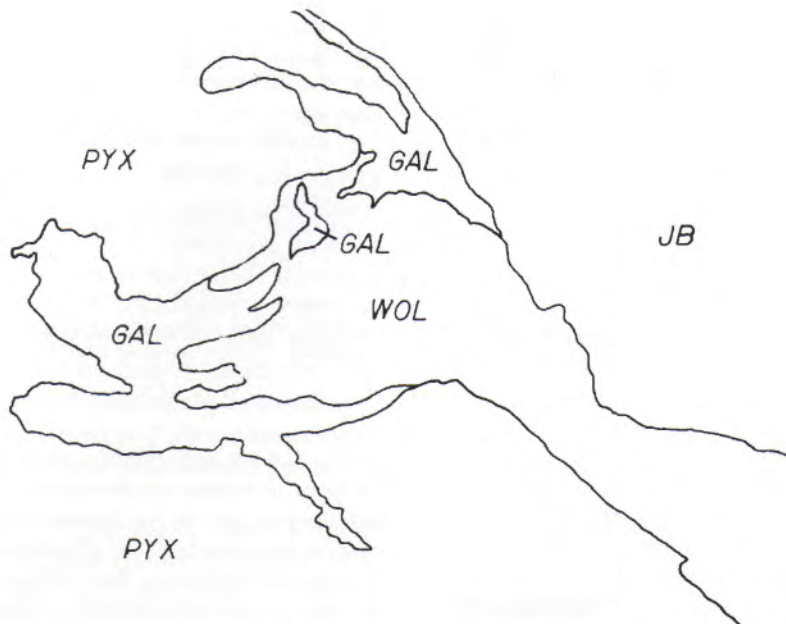


Figure 2b. Explanation of 2a, Wol - wollastonite-bearing rock, Pyx - pyroxene calcisilicate rock, Gal - galena-sphalerite segregations in pyroxene-microcline calcisilicate rock, and Jb - area of cross-cutting veinlets.

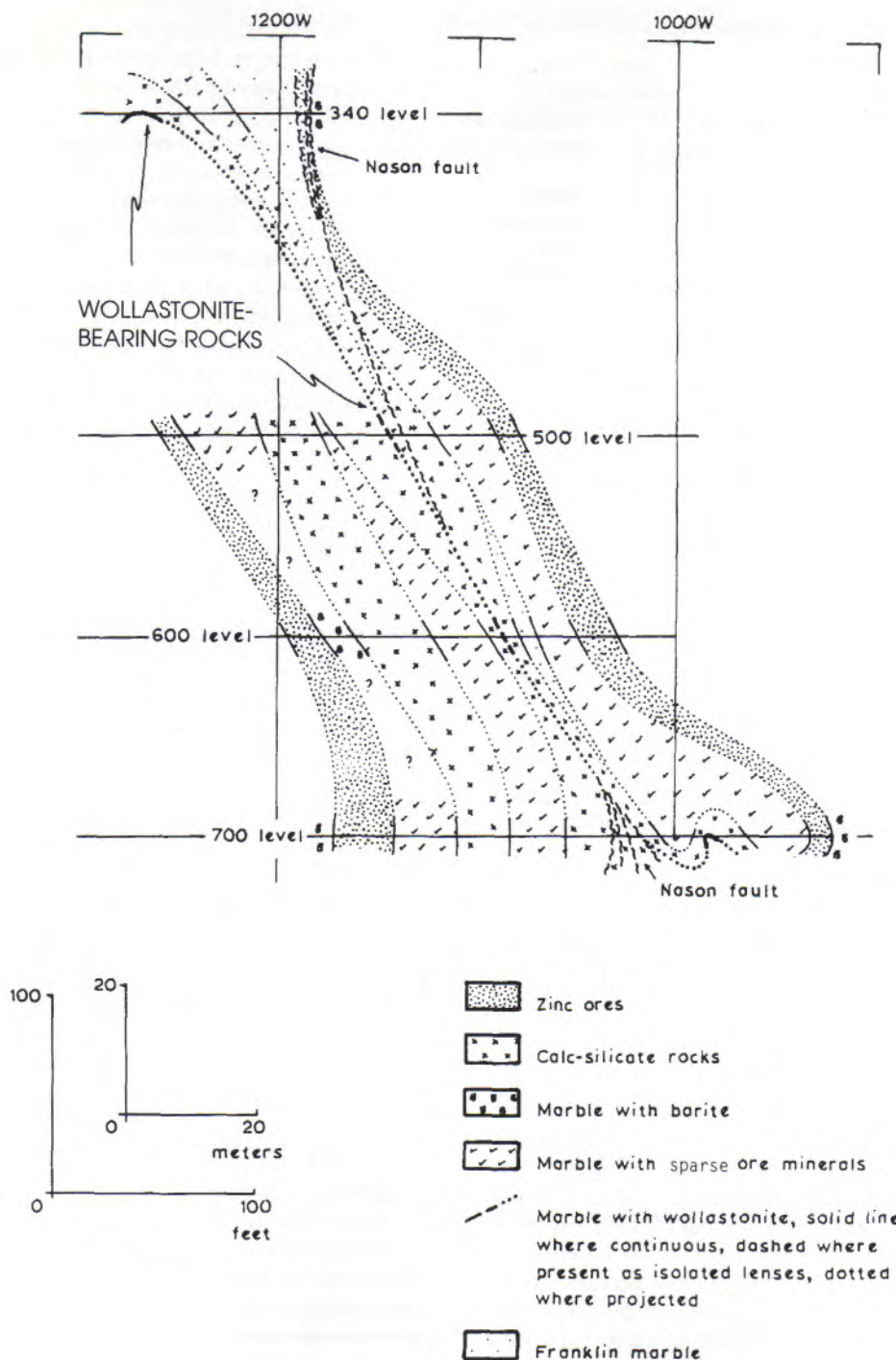


Figure 3. Interpretive vertical cross-section at 700N, Sterling Mine, New Jersey, looking north. The cross-section shows the relative positions of wollastonite-bearing rocks, associated pyroxene calc-silicate rocks, and Nason Fault.

wollastonite-bearing rock. Elsewhere, the calc-silicate rock appears unfoliated. Bordering the calc-silicate unit on both sides in the crosscut are bodies of the impure marble unit. Cutting the calc-silicate body at the upper right of Figures 2a,b is a set of narrow fractures which host the veinlet assemblage. Veinlets range up to 1 cm in thickness but average about 6 mm. They strike NE and dip at a shallow angle to the southeast. Veinlets are

generally completely filled but locally open into flattened vugs several mm in length, in which are deposited euhedral crystals of johnbaumite and piemontite, together with barite, epidote, rhodonite, and other minerals. Fractures hosting the veinlet assemblage are continuous from calc-silicate rock to marble and the wollastonite-bearing rock but are poorly developed in the latter two and are devoid of piemontite, johnbaumite, barite, or rhodon-

Table 1. General mineralogy of the veinlet, selvage, and wallrock assemblages

Veinlet	Selvage	Pyroxene Calcsilicate	Wollastonite- Bearing Rock
Andradite	Calcite	Calcite	Calcite
Calcite	Epidote	Galena	Fluorapatite
Celestite	Microcline	Hedenbergite	Galena
Chabazite	Phlogopite	Microcline	Grossular(?)
Epidote	Sphalerite	Hedenbergite	
Fluorite	Phlogopite		
Galena	Quartz		
Johnbaumite	Sphalerite		
Microcline (?)	Willemite		
Monohydrocalcite	Wollastonite		
Phlogopite			
Piemontite			
Rhodonite			

(?) - EDS indication only, no X-ray validation

ite. All of these minerals disappear abruptly at the wollastonite-rich rock and marble contacts. Internal structure of the veinlets is crustiform and generally symmetrical. Most veinlets are rimmed on both sides by selvages, averaging about 4 mm in thickness, of manganiferous epidote with traces of other minerals. Selvage zones and veinlets are distinct in many examples, but in some, epidote is intergrown and apparently contemporaneous with veinlet barite. Epidote also fills the extensions of the veinlets into the marble and wollastonite-rich rock. Where some fractures containing the veinlet assemblage pass into the wollastonite-bearing rock, the piemontite and/or rhodonite are altered to an unidentified brown substance. Figure 3 is a vertical cross-section, oriented E-W and drawn at the 700N datum of the NJZC coordinate system, showing the wollastonite-rich rock and associated rocks, together with the Nason Fault and the zinc deposit, from 340 through 700 Levels. Illustrated elements are projected orthogonal to the plane of the section, over a distance of 12.2 m or less. This section is interpretive, and other constructions of geologic relations at 700N might be made. Implicit in this interpretation are, for instance, the assumptions that the wollastonite-bearing rocks of the keel represent a single unit, and that those exposed on 700 Level in the east block of the Nason Fault represent the same unit as is exposed in the west block of the fault on 500 and 340 Levels. This construction provides a plausible portrayal, however, for all of the observed structural orientations of contacts, foliation, and the Nason Fault in this part of the keel area. This interpretation represents the wollastonite-bearing rocks and associated zone of pyroxene calcsilicate rocks on 700 Level as a S-shaped fold which may be related to dragging in the downdropped east block of the Nason Fault. Fractures hosting the veinlet assemblage are tangential to the nose of one element of this fold and might therefore represent extensional features, opened during the folding and faulting episode. Alternatively, the fractures hosting the veinlet assemblage may be unrelated to movement on the Nason Fault or any folding event. These possibilities may be resolved by the detailed structural studies of Earl Verbeek and Marilyn Grout.

MINERALOGY

With the noted exceptions, all species herein reported were confirmed by X-ray powder photography, using a 114-mm Gandolfi camera, or by X-ray bulk diffractogram, both on a modified Philips Automated X-ray Diffractometer with DEC Vax II hardware control. Veinlet and selvage minerals, as well as the apatites of the wollastonite-bearing rock, were identified by powder photographic method and other species by diffractogram. All species were also studied by SEM-EDS methods, using a JEOL JSM-840 scanning electron microscope (SEM) or a JEOL JXA-35 electron probe microanalyzer, both equipped with KEVEX EDS (energy dispersive spectra) detector. Semiquantitative chemical analyses reported for several species were performed with the microprobe using the TRACOR "SQ" semiquantitative analysis program with DEC PDP-11/73 hardware control. This program utilizes EDS data and applies ZAF corrections, iterating as necessary to achieve best fit with the line-energy intensity library, which is part of the program file. Lines used for analysis are operator-selected, and degree of fit is measured by means of Chi-squared statistical test. The ideal test value is unity. Chi-squared values which are less than 2.5 represent good quality

analyses by comparison to quantitative analyses for the same samples. Deviations from unity generally result from irregularities in the specimen surface or from failure of the operator to specify all of the X-ray energies present in the spectrum. It is sometimes very difficult, for instance, for the operator to distinguish the X-ray lines of trace constituents from the background continuum. All analyses were performed with 200 second counting time at an operating voltage of 25 kV. Shortwave ultraviolet fluorescence response was checked using an UVP Inc. UVG-54 lamp. Thirteen specimens were examined, only one of which was precisely located. Studied specimens were derived from the following collections: ST-series, reference collection of the Sterling Hill Mining Museum, J-series, author's personal collection, and JE, one specimen from the collection of Mr. John Ebner. Table 1 shows the general mineralogy of the locality, divided into veinlet, selvage, pyroxene calcsilicate rock, and wollastonite-bearing rock assemblages. Selected species are described in detail below.

VEINLET AND SELVAGE MINERALS

Barite BaSO₄

Barite is the most abundant phase of the veinlet assemblage. It occurs generally as white massive material, intergrown with johnbaumite, andradite, and, near veinlet walls, epidote. More rarely, in vugs, it is present as white to blue-grey tablets, averaging about 0.1 mm in maximum dimension. Some barite contains 2-5 μm inclusions of a second species, which may be barian microcline. The chemical composition of this included species suggests a potassium feldspar with minor Ba, but it has not been confirmed by X-ray diffraction. Because of the minute size of the inclusions, there is also question as to the origin of Ba lines in the energy-dispersive spectrum. The electron beam may be exciting Ba from the barite matrix. Barite from the veinlet assemblage does not appear to fluoresce in shortwave ultraviolet radiation, but a response may be obscured by the intense fluorescence of johnbaumite.

Celestite SrSO_4

Celestite was observed on a single hand specimen (J9236). It is present as parallel aggregates of corroded single crystals and crude twins, with individuals averaging about 15 μm in maximum dimension. These are implanted on calcite and barian microcline with barite, epidote, and subhedral galena in an open veinlet. The wall rock of the veinlet is pyroxene calcsilicate, but the veinlet is unusual in that there are no selvage zones.

Chabazite $\text{CaAl}_2\text{Si}_4\text{O}_{12} \cdot 6\text{H}_2\text{O}$

Chabazite also occurs on a single specimen (JE-2) as a few frosted and very pale yellow pseudorhombhedra ranging from 0.5 to 2 mm in maximum dimension, on epidote and calcite in an open veinlet. Thin epidote selvages border the veinlet. The same hand specimen also exhibits several very thin veinlets completely filled with epidote and piemontite.

Epidote $\text{Ca}_2(\text{Fe,Al})_3(\text{SiO}_4)_3(\text{OH})$

Epidote, as typical pistachio green masses, is the major constituent of the selvage zones. Selvage epidote forms tightly interlocking mosaics of 0.5 to 3 mm prisms, which appear to have replaced hedenbergite and possibly barian microcline. Epidote in some filled veinlets grades into piemontite, as shown by gradual change from green to pink color. In most specimens, minerals of the veinlets are implanted on selvage epidote. Epidote in a few samples also occurs as euhedral prisms, averaging about 0.2 mm in length, that project from the massive mineral into cavities in veinlet interiors. Euhedral epidote is locally coated with barite, piemontite, johnbaumite, and calcite, but more commonly the crystals are uncoated. The epidote is manganiferous (Table 2).

Johnbaumite $\text{Ca}_3(\text{AsO}_4)_3(\text{OH})$

Johnbaumite is less abundant than either barite or piemontite in the veinlet assemblage, but in one 3x3x5 cm specimen (J9122) constitutes about half of the veinlet filling. Most of the johnbaumite is white and granular, intergrown with barite and piemontite in filled veinlets. More rarely, the mineral is present as hexagonal,

barrel-shaped crystals with skeletal terminations, very similar to some pyromorphite. The crystals project into vugs and average about 50 μm in length. A few johnbaumite crystals reach 200 μm in length and are visible with the binocular microscope. Johnbaumite fluoresces intense medium orange in shortwave ultraviolet radiation. The massive mineral from the site resembles the johnbaumite of the Franklin type description (Dunn *et al.*, 1980). Johnbaumite was identified by a combination of X-ray diffraction and chemical-analytical techniques. X-ray powder photograph indicated a member of the apatite group. EDS scan revealed As >> P with only trace quantities of Cl in several grains. Wavelength-dispersive analysis of the same grains at the F K- α line revealed similar trace amounts of fluorine. The mineral was therefore identified as the hydroxyl-dominant arsenate-apatite, johnbaumite.

Monohydrocalcite $\text{CaCO}_3 \cdot \text{H}_2\text{O}$

Monohydrocalcite was identified on only one specimen (ST700-740XC-5). It occurs as microbotryoidal crusts on calcite and epidote in a portion of an open veinlet. It is white and earthy with no distinguishable internal structure in visible light but fluoresces intense, pale green in shortwave ultraviolet radiation.

Piemontite $\text{Ca}_2(\text{Al,Mn,Fe})_3(\text{SiO}_4)_3(\text{OH})$

The manganese epidote piemontite is most common as pale pink masses with barite or epidote, the three minerals completely filling host fractures. Less commonly, piemontite occurs as brighter pink prismatic crystals projecting into open vugs. Piemontite crystals average about 0.25 mm in length and are associated with barite and johnbaumite. Where well-crystallized, piemontite is readily distinguished from rhodonite by crystal morphology and cleavage of the piemontite. A mineral with chemical composition corresponding to piemontite was first noted during SEM-EDS study of chips from veinlet samples. The species was later verified by X-ray powder photography. A semi-quantitative chemical analysis of piemontite is given in Table 2, together with analyses of epidote.

Rhodonite MnSiO_3

Rhodonite is not as abundant in the veinlet assemblage as piemontite, johnbaumite, or barite. Rhodonite occurs as bright pink prisms averaging about 0.3 mm in length. It encrusts the other three minerals and is itself locally encrusted by calcite.

ROCK-FORMING MINERALS**Apatite** $\text{Ca}_5(\text{PO}_4)_3(\text{F,OH})$

Apatite is apparently a widespread component of the wollastonite-bearing rocks, but it occurs only in minor quantities. It is present as pale to medium grey, translucent, anhedral grains averaging about 0.5 mm in maximum dimension. These are mostly disseminated in calcite, but are locally found in wollastonite. The mineral contains variable but significant quantities of As (Table 3). The relatively lower As value for sample ST700-740XC-4, collected by Richard Bostwick at the margin of the pod of wollastonite-bearing rock at approximate mine coordinates - 1688,739N,986W, may indicate depletion in As in the apatites from the pod margin. Although the analyzed chips appeared megascopically fresh, the consistently low cation:anion ratios suggest also that they may be relatively depleted in the metals Ca, Fe, and Mn. All specimens were checked for the presence of C

Table 2. Semi-quantitative chemical analyses of epidote and piemontite

(all values in wt.%; normalized to 100%)

Sample#	ST-5(1)	ST-5(2)	J9122(3)
Al_2O_3	9.4	8.0	7.2
SiO_2	28.1	33.0	29.0
CaO	44.4	32.9	38.0
MnO	0.6	4.1	21.4
FeO	17.5	22.0	4.4
Total	100.0	100.0	100.0

(1) - Sample ST700-740XC-5, massive epidote from selvage zone. Analysis is average of 5 spots; Chi-square = 2.67

(2) - Sample ST700-740XC-5, euhedral epidote from vug along veinlet. Analysis is average of 4 spots; Chi-square = 1.88

(3) - Euhedral piemontite from vug along veinlet. Analysis is average of 5 spots; Chi-square = 2.38

Table 3. Semi-quantitative chemical analyses of apatite

(all values wt.%; normalized to 100%)

Sample#	J9082(1)	J9242(2)	ST-4(3)
SiO ₂	3.8	3.8	n.d.
SO ₃	3.6	2.9	n.d.
Cl	2.0	1.9	0.1
CaO	65.2	64.5	69.2
P ₂ O ₅	10.9	8.5	16.4
MnO	0.1	0.2	n.d.
FeO	0.1	0.1	0.2
As ₂ O ₅	14.3	18.1	14.1
Total	100.0	100.0	100.0

n.d. - Not detected

- (1) - Sample from interior of pod of wollastonite-bearing rock. Analysis is average of 5 spots, Chi-square = 3.02.
- (2) - Sample from interior of pod of wollastonite-bearing rock. Analysis is average of 5 spots, Chi-square = 2.75.
- (3) - Sample ST700-740XC-4, from margin of pod of wollastonite-bearing rock; apatite grain in contact with epidote selvage. Analysis is average of 4 spots, Chi-square = 2.72.

(CO₃), using a MYRLOD layered analyzing crystal and the microprobe wavelength capability, but they contain only traces. The presence of significant F was also shown using the microprobe wavelength function, but the ratio F:OH could not be measured. The species is therefore verified only as apatite.

Hedenbergite Ca(Fe,Mg,Mn)Si₂O₆

Pyroxene of the pyroxene calcsilicate rock is present as a tightly interlocking mosaic of 2-8 mm subhedral grains. It is hedenbergite with approximate composition, calculated in terms of end-members, Hd₅₀Di₄₀Jo₁₀ (Table 4, Hd = hedenbergite, Di = diopside, Jo = johannsenite). Analyzed pyroxene chips were taken from hand specimens, containing sections of veinlets and selvages.

Microcline (K,Ba)Al₁₋₂Si₃₋₂O₈

Microcline comprises 10-20 vol% of pyroxene calcsilicate samples that, judging from their prominent foliation, were apparently collected in close proximity to the pod of wollastonite-bearing rock. The mineral is rare, however, in unfoliated pyroxene calcsilicate specimens. Microcline is present in the foliated samples as 2-15 mm subhedral grains, which commonly appear to have replaced hedenbergite. The microcline is barian with approximate composition, calculated in terms of end-members, Mc₉₃Cs₇ (Table 5, Mc = microcline, Cs = celsian).

DISCUSSION

Secondary minerals which post-date metamorphism of the zinc deposit and its enclosing rocks are numerous in the impressive list of species found at Sterling Hill, New Jersey. The veinlet

Table 4. Semi-quantitative chemical analyses of pyroxene

(all values in wt.%; normalized to 100%)

Sample#	J9235(1)	J9236(2)	J9447(3)
Na ₂ O	0.5	0.5	0.5
MgO	7.0	7.3	7.2
Al ₂ O ₃	1.3	1.2	1.2
SiO ₂	38.9	38.6	38.2
CaO	27.5	27.7	27.7
TiO ₂	0.1	0.1	n.d.
MnO	4.0	4.4	4.2
FeO	20.7	20.2	21.0
Total	100.0	100.0	100.0

n.d. - Not detected

- (1) - Sample from margin of pyroxene calcsilicate zone; contains abundant calcite and microcline and is strongly foliated. Analysis is average of 4 spots; Chi-square = 1.66.
- (2) - Sample taken 3.5 cm from open veinlet with barite, galena, celestite, etc. Analysis is average of 5 spots; Chi-square = 1.52.
- (3) - Sample taken 4 cm from veinlet filled with epidote and piemontite. Analysis is average of 5 spots; Chi-square = 1.68.

Table 5. Semi-quantitative chemical analyses of microcline

(all values in wt.%; normalized to 100%)

Sample#	J9235*
K ₂ O	13.0
Al ₂ O ₃	0.8
SiO ₂	79.4
BaO	6.8
Total:	100.0

*Sample from margin of pyroxene calcsilicate zone; contains abundant calcite and hedenbergite and is strongly foliated. Analysis is average of 6 spots; Chi-square = 1.22.

assemblage described in this report is, however, unlike others reported in the literature on this deposit. It is unusual because of the inclusion of yet another phase new to this remarkable locality, but given the bulk chemistry of Sterling Mine ores and wall rocks, the occurrence of piemontite can perhaps be taken as no great surprise. It is more unusual certainly because of the inclusion of a rare apatite-group mineral, johnbaumite, which has clearly been formed by some secondary process. Most of the apatites at Sterling Hill appear to be cogenetic with the ore minerals. It is therefore interesting to consider the origin of the assemblage. Minerals of the veinlet assemblage have been formed largely by open space filling, as indicated by crustiform structure and the

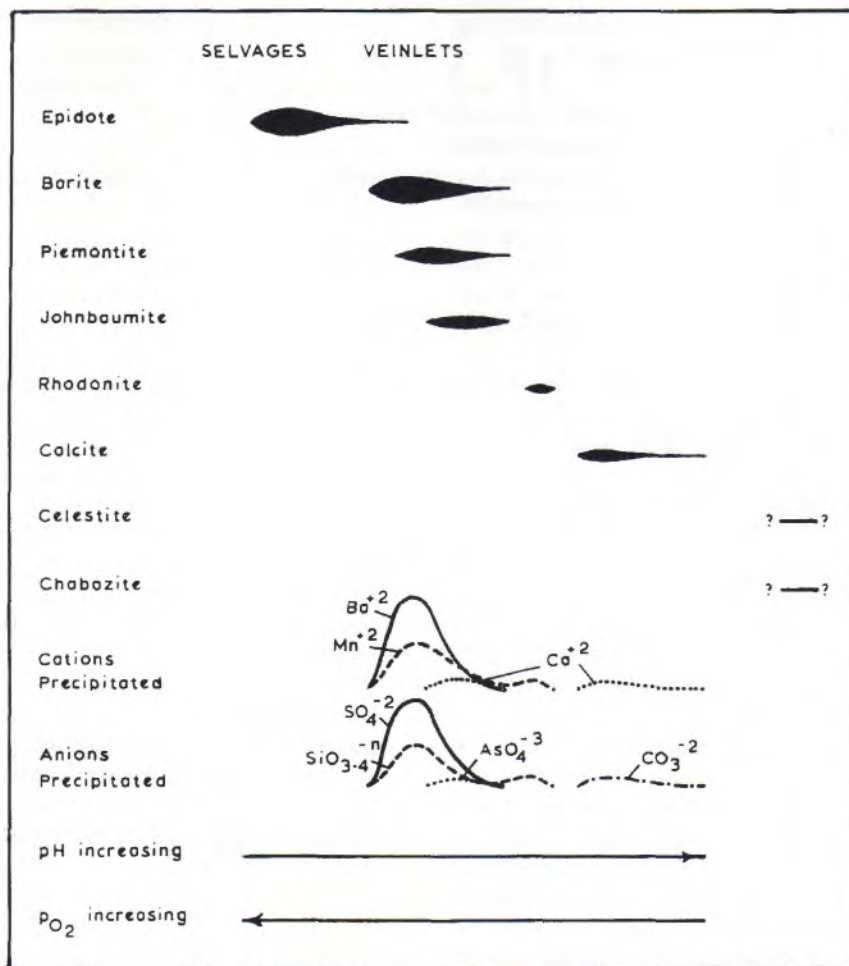
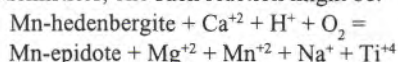


Figure 4. Mineral paragenesis of the veinlet assemblage (minor species or those for which paragenetic evidence is equivocal are omitted). Figure also shows chemical species precipitated and qualitative changes in solution composition with time.

locally vuggy nature of the veinlets. Species of the selvage zones on the other hand, have been formed by replacement of the original wallrock. The observation that all of the veinlet-filling species were deposited on epidote shows that formation of the selvages at least began before deposition of the minerals in the veinlets. Intergrowths of epidote with barite and the presence of euhedral epidote in cavities indicate that some epidote deposition accompanied formation of the veinlet minerals. Common and consistent encrustations of some veinlet minerals upon others provide much additional evidence of the sequence of mineral deposition. Paragenesis of the veinlet assemblage is thus readily defined as shown in Figure 4. Crustiform structure and selvages bordering veins have long been regarded as strong evidence of mineral deposition from an aqueous fluid, or hydrothermal phase (e.g. Lindgren, 1928; Cathles, 1991). The paragenetic diagram of Figure 4 therefore also illustrates some of the changes which a mineral-depositing, hydrothermal fluid would have undergone with time: cations and anions precipitated, change in pH, and change in oxidation state. Changes in cations and anions precipi-

tated are deduced from the chemistry of minerals formed. Changes in pH and oxidation state are deduced from the nature of the anions incorporated into successively forming mineral species. Sulfates and arsenates form at acid to neutral pH and relatively high oxidation state; carbonates and silicates are stable at generally lower oxidation state and neutral to alkaline pH (Barnes, 1979). The diagram does not account for either celestite or chabazite, both of which may well have formed during subsequent and unrelated mineralizing event(s). The highly localized nature of the veinlet assemblage, its confinement to the pyroxene calcisilicate rocks and disappearance where host fractures pass into other rock types, offer strong argument for local sources of metals. Specifically, these are: Mn, Fe, and Al from hedenbergite in the calcisilicate rocks; Ba from barian microcline in the same rocks; and As from apatite of the wollastonite-bearing rock. Because hedenbergite obviously has been converted to epidote along the selvage zones, it is instructive to write a chemical reaction for the

epidotization process. Although generalized because of uncertain mineral chemistries, one such reaction might be:



Quartz is not present in the assemblage, so silica is neither reactant nor product. Although epidote is manganiferous, the reaction liberates additional Mn to form piemontite and rhodonite. The reaction is favored by acid and oxidizing conditions and consumes both oxygen and hydrogen ions. As a reaction of this type progresses it would therefore tend to raise solution pH and lower oxidation state. The consistency of the chemical analyses of hedenbergite (Table 4) in proximity to the veinlets perhaps suggests that the only local source of Mn lay within the selvage zones; and thus that transport distances for Mn in solution were relatively short, on the order of centimeters. Transport distances for Ba from barian microcline would have been similar. If As in johnbaumite was derived from reworking of arsenian apatites in the wollastonite-bearing rocks, however, transport distances for As must have been somewhat greater, on the scale of meters. Few of the veinlets contact the wollastonite-bearing rocks. It is also instructive to consider the hedenbergite-epidote reaction in another way. Utilizing ideal unit cell data for calculation (Deer *et al.*, 1966) and assuming ideal compositions, whereby 3 moles of hedenbergite yields 2 moles of epidote, the reaction leads to a 27% volume reduction: 1.0 m³ of hedenbergite produces 0.73 m³ of epidote. This might account for production of additional open space along fractures to provide for the deposition of johnbaumite and other minerals. Hydrothermal activity would certainly have had to succeed opening of the original host fractures, whether or not they were enlarged by replacement. If the fractures are indeed, extensional features related to drag folding and down-drop of the east block of Nason Fault, mineralization would also have to postdate the fault. Metsger (1990) has stated, however, that the age of the Nason Fault is uncertain. Verbeek (written communication, 1993) has stated furthermore that the Nason Fault has undergone at least 3 episodes of slip. The timing of formation of the veinlet assemblage is thus unknown.

ACKNOWLEDGMENTS

Many individuals and institutions contributed to the preparation of this report. The author is grateful to both the Sterling Hill Mining Museum and to E. I. DuPont de Nemours & Company for permission to publish these results. Earl Verbeek, Steven Misiur, Robert Hauck, John Kolic, Richard Bostwick, and Chester Lemanski are thanked for the information, on which the geologic section of the report is so dependent. John Ebner is acknowledged for access to the single chabazite specimen from the locality. The author is also grateful to Gary Grenier for specimen photography. DuPont personnel, Chip Michel, Joseph Brennan, Ulrich Klabunde, Richard Harlow, and Dennis Redmond are thanked for access to instruments and assistance in their use. Wallace L. Kremer is acknowledged for management support. The author is grateful to Pete J. Dunn and Earl Verbeek for their careful reviews, which materially improved the paper. He also wishes to acknowledge Nadir L. Jenkins for preparation of the final typescript.

REFERENCES

- Barnes, H.L., ed. (1979) *Geochemistry of hydrothermal ore deposits*. 2nd Edition, Wiley-Interscience, New York, 798 p.
- Cathles, L.M. (1991) The importance of vein selvaging in controlling the intensity and character of subsurface alteration in hydrothermal systems. *Economic Geology*, **86**, 466-471.
- Deer, W.A., Howie, R.A., and Zussman, J. (1966) *An introduction to the rock forming minerals*: New York, Wiley, 528 p.
- Dunn, P.J., Peacor, D.R., and Newberry, N. (1980) Johnbaumite, a new member of the apatite group from Franklin, New Jersey: *American Mineralogist*, **65**, 1143-1145.
- Lindgren, W. (1928) *Mineral deposits*. McGraw-Hill Book Company, New York, 3rd Ed., 1049 p.
- Metsger, R.W. (1990) Geology of the Sterling Hill Zn, Fe, Mn, deposit, in *Character and origin of the Franklin-Sterling Hill orebodies*. Proceedings Volume. Lehigh University, Bethlehem, May 19, 1990, 32-48.
- Metsger, R.W., Tennant, C.B., and Rodda, J.L. (1958) Geochemistry of the Sterling Hill zinc deposit, Sussex County, New Jersey. *Geological Society of America Bulletin*, **69**, 775-788.
- Sanford, S. (1992) *Franklin-Sterling Hill mining terms: a primer for the novice*. *The Picking Table*, **33**, no. 2, 14-19.





PUBLICATIONS AVAILABLE

FROM THE FRANKLIN-OGDENSBURG MINERALOGICAL SOCIETY, INC.



THE PICKING TABLE

Complete Set of *The Picking Table*

(Volume 1, #1 through the current issue)

set..... \$85.00 (+\$6.00 UPS fee)

Individual back-issues of *The Picking Table*

Volume 1, #1 through volume 23, #2: each issue.....\$2.50
Volume 24, #1 through volume 29, #2: each issue.....\$3.50
Volume 30, #1 through volume 34, #2: each issue.....\$5.00

(Add \$0.75 for issues through vol. 23, #2; and \$1.00 for issues beginning with vol. 24, #1 for postage)

Note: All issues of *The Picking Table* prior to volume 23 are available only as *photocopies*.

Books and other publications

Palache, Charles (1935) *The Minerals of Franklin and Sterling Hill, New Jersey.*

U.S. Geological Survey Professional paper 180, 135pp. Soft-cover, FOMS reprint 1974.

\$10. (+\$2.50 postage)

Fron del, Clifford and Baum, John L. (1974) *Structure and Mineralogy of the Franklin Zinc-Iron*

Manganese Deposit, New Jersey. Economic Geology, 69, 2, pp. 157-180. Photocopies only are available.

\$2.50 (+\$1.25 postage)

Horuzy, Paul (editor) (1990) *The Odyssey of Ogdensburg and the Sterling Zinc Mine.*

Privately printed, Sterling Hill Mining Company.

\$6.50 (+\$1.75 postage)

Shuster, Elwood D. (1927) *Historical Notes of the Iron and Zinc Mining Industry in Sussex County,*

New Jersey. Privately printed. Franklin Mineral Museum reprint.

\$3.00 (+\$0.75 postage)

Proceedings Volume, Lehigh-FOMS Symposium (1990): *Character and Origin of the Franklin-Sterling Hill Orebodies*, 118pp.

\$12.50 (+\$2.50 postage)

The Henkel Glossary of Fluorescent Minerals.

Journal of the Fluorescent Mineral Society, Special Issue, volume 15 (1988-89).

\$12.50 (+\$1.75 postage)

Most publications are made available at Society meetings. However, if ordering by mail, make check or money order payable to FOMS, and address your order to:

Mr. Steven C. Misiur, Asst. Treasurer FOMS
309 Fernwood Terrace,
Linden, NJ 07036

**FRANKLIN-OGDENSBURG
MINERALOGICAL SOCIETY, INC.**

BOX 146 - FRANKLIN, NEW JERSEY 07416

